Virus-Induced Interferon- Causes Insulin Resistance in Skeletal Muscle and Derails Glycemic Control in Obesity

Šestan, Marko ; Marinović, Sonja ; Kavazović, Inga ; Cekinović, Đurđica ; Wueest, Stephan ; Turk Wensveen, Tamara ; Brizić, Ilija ; Jonjić, Stipan ; Konrad, Daniel ; Wensveen, Felix M ; Polić, Bojan

Abstract: Pro-inflammatory cytokines of a T helper-1-signature are known to promote insulin resistance (IR) in obesity, but the physiological role of this mechanism is unclear. It is also unknown whether and how viral infection induces loss of glycemic control in subjects at risk for developing diabetes mellitus type 2 (DM2). We have found in mice and humans that viral infection caused short-term systemic IR. Virally-induced interferon- (IFN-) directly targeted skeletal muscle to downregulate the insulin receptor but did not cause loss of glycemic control because of a compensatory increase of insulin production. Hyperinsulinemia enhanced antiviral immunity through direct stimulation of CD8 effector T cell function. In pre-diabetic mice with hepatic IR caused by diet-induced obesity, infection resulted in loss of glycemic control. Thus, upon pathogen encounter, the immune system transiently reduces insulin sensitivity of skeletal muscle to induce hyperinsulinemia and promote antiviral immunity, which derails to glucose intolerance in pre-diabetic obese subjects. VIDEO ABSTRACT.

DOI: https://doi.org/10.1016/j.immuni.2018.05.005

TITLE

Virus-induced interferon-γ causes insulin resistance in skeletal muscle and derails glycemic control in obesity

AUTHORS

Marko Šestan[1], Sonja Marinović[1,7], Inga Kavazović[1,7], Đurđica Cekinović[2], Stephan Wueest[3], Tamara Turk Wensveen[4], Ilija Brizić[5], Stipan Jonjić[1, 5], Daniel Konrad[3], Felix M. Wensveen[1,8] and Bojan Polić[1,6, 8*]

[1]Department of Histology and Embryology, Faculty of Medicine, University of Rijeka, Rijeka, Croatia

[2] Department of Infectology, Clinical Hospital Center Rijeka, Rijeka, Croatia

[3] Division of Pediatric Endocrinology and Diabetology and Children's Research Centre, University Children's Hospital, Zurich, Switzerland

[4]Department of Endocrinology, Clinical Hospital Center Rijeka, Rijeka, Croatia

[5]Center for proteomics, Faculty of Medicine, University of Rijeka, Rijeka, Croatia

[6]Lead contact

[7, 8] Equal contribution

[*] Corresponding author. Email: bojan.polic@medri.uniri.hr

SUMMARY

Pro-inflammatory cytokines of a T helper-1-signature are known to promote insulin resistance (IR) in obesity, but the physiological role of this mechanism is unclear. It is also unknown whether and how viral infection induces loss of glycemic control in subjects at risk for developing diabetes mellitus type 2 (DM2). We have found in mice and humans that viral infection caused short-term systemic IR. Virally-induced interferon-γ directly targeted skeletal muscle to downregulate insulin receptor but did not cause loss of glycemic control because of a compensatory increase of insulin production. Hyperinsulinemia enhanced antiviral immunity through direct stimulation of $CD8^+$ effector T cell function. In pre-diabetic mice with hepatic IR caused by diet-induced obesity, infection resulted in loss of glycemic control. Thus, upon pathogen encounter, the immune system transiently reduces insulin sensitivity of skeletal muscle to induce hyperinsulinemia and promote antiviral immunity, which derails to glucose intolerance in pre-diabetic obese subjects.

INTRODUCTION

Diabetes mellitus type 2 (DM2) is a highly prevalent (Stevens et al., 2012) metabolic disease, characterized by high blood glucose concentrations. The pathology of DM2 involves many organs but its main underlying mechanism is decreased insulin sensitivity of the liver and skeletal muscle and an inability of pancreatic β-cells to compensate for this defect (Defronzo, 2009). DM2 is diagnosed based on increased concentrations of glycosylated hemoglobin (HbA1c), fasting plasma glucose (FPG) or postprandial blood glucose (American Diabetes, 2018). If these concentrations are increased, but do not reach DM2 threshold values, people are diagnosed with pre-diabetes (Abdul-Ghani et al., 2006). Prospective studies show that changes in glycemic control occur gradually over years, but typically contain an abrupt increase in metabolic parameters preceding diagnosis of DM2 (Mason et al., 2007; Tabak et al., 2012). Progression from pre-diabetes to DM2 therefore appears to involve an unknown "event" that pushes systemic insulin resistance (IR) beyond the ability of the pancreas to compensate. DM2 is associated with chronic systemic low-grade inflammation originating in visceral adipose tissue (VAT) (Wensveen et al., 2015b). Obese VAT accumulates pro-inflammatory immune cells and drives a Type-1 immune response, normally associated with viral infection, characterized by the production of cytokines such as tumor necrosis factor (TNF) and interleukin 1β (IL-1β) (Johnson et al., 2012; Wensveen et al., 2015a; Wensveen et al., 2015b). Obesity thus mimics a state of chronic systemic low-grade infection and leakage of pro-inflammatory cytokines into circulation is thought to contribute to systemic IR (Johnson et al., 2012; Wensveen et al., 2015b). Acute infection may therefore represent the "event" that drives rapid progression to DM2 in pre-diabetes. Only few epidemiological studies address this topic and these do suggest that infection is associated with a higher risk of DM2 (Chen et al., 2012; Leinonen and Saikku, 1999; Roberts and Cech, 2005). However, direct experimental evidence if and how infection impacts glycemic control are lacking.

It is currently unclear what the physiological role is of reduced systemic insulin sensitivity following infection. Immune activation comes at a considerable energetic cost (Ganeshan and Chawla, 2014), as cells switch from oxidative to glycolytic metabolism (O'Neill et al., 2016). It was therefore proposed that inflammation-induced IR is a physiological response to infection that aims to increase systemic glucose availability to activated immune cells (Kotas and Medzhitov, 2015). However, infection-induced acute loss of glycemic control is only observed under extreme conditions such as sepsis, whereas DM2 is associated only with low amounts of systemic inflammation (Johnson et al., 2012; Marik and Raghavan, 2004).

Alternatively, inflammation-induced IR may be a strategy of the immune system to involve endocrine mediators in the response against infection. Both cytokines and hormones regulate the metabolism of cells in response to alterations in the external environment. Frequently their receptors overlap both in the intracellular signaling pathways that they use and the effects that they mediate (Ouchi et al., 2011). For example, receptors for both IL-6 and for the adipose tissue-derived hormone leptin signal through the Jak2-Stat3 signaling pathway (Heinrich et al., 2003; Munzberg and Morrison, 2015) and both molecules promote proliferation of immune cells and excretion of cytokines by macrophages (Heinrich et al., 2003). The insulin receptor shares its downstream signaling cascade with CD28, one of the most potent costimulatory molecules for $CD8^+$ T cells (Pessin and Saltiel, 2000; Sharpe and Freeman, 2002). Both pathways converge on phosphatidylinositol 3 kinase (PI3K), enhancing anabolic metabolism and increasing glucose transporter amounts on the cell membrane (Frauwirth et al., 2002; Pessin and Saltiel, 2000). IR is associated with hyperinsulinemia. Whether insulin plays a role in promoting immune responses following infection is unknown.

Here, we investigated how infection impacts insulin-mediated regulation of glycemia. We found that virally-induced IFNγ caused IR in the skeletal muscle through direct engagement of the IFN-γ receptor on myocytes and down-modulation of the insulin receptor on these cells. Infection-induced selective IR drove an increase of systemic insulin concentrations to prevent hyperglycemia, but also to boost the anti-viral $CD8^+$ T cell response through direct promotion of effector cell function. When systemic insulin sensitivity is already reduced, such as in pre-diabetic obese subjects due to hepatic IR, infection overwhelmed the ability of the endocrine system to compensate for increased muscle IR and glucose intolerance (GI) ensues. We thus identify an immune-endocrine regulatory feed-back mechanism of antiviral immunity and provide additional insights in the underlying physiology of DM2.

RESULTS

Viral infection causes development of insulin resistance, but not glucose intolerance

First, we investigated whether infection impacts systemic metabolic parameters in humans. Body mass index (BMI) and blood parameters were obtained from euglycemic people with normal weight (BMI of 18-25 kg/m^2) and overweight (BMI >25), diagnosed with acute respiratory infection at time of presentation of symptoms and three months later. Infection transiently increased fasting plasma insulin (FPI) in both groups (**Figure 1A**). In contrast, FPG

was not significantly affected by infection (**Figure 1B**). Notably, the homeostasis model assessment – insulin resistance (HOMA-IR) index values, which inversely correlate with systemic insulin sensitivity, were increased during acute infection, especially for people with overweight (**Figure 1C**). Thus, acute infection appeared to transiently decrease systemic insulin sensitivity in humans, without affecting blood glucose concentrations.

We next used murine cytomegalovirus (MCMV) as an animal model for a common human infection (Krmpotic et al., 2003). MCMV has a broad tropism, including key organs involved in the regulation of glucose homeostasis, such as liver, VAT, pancreas and skeletal muscle (**Figure 1D**). Animals were infected with MCMV and after seven days subjected to an insulin tolerance test (ITT). We observed that MCMV infection resulted in transient intolerance to insulin (**Figure 1E; S1A**). To confirm that this effect was the result of IR, mice were subjected to hyperinsulinemic-euglycemic clamping on day five after infection. Indeed, infected animals showed a strongly reduced sensitivity to insulin in comparison to non-infected controls (**Figure 1F**; **S1B**), as determined by a lower glucose infusion rate (GIR). To determine whether infection-induced IR resulted in loss of glycemic control, infected animals were analyzed by glucose tolerance test (GTT). Despite IR, infection did not result in GI (**Figure 1G**). As in humans, infection was associated with elevated FPI concentrations. Moreover, following glucose challenge, increased insulin production was observed in infected animals, explaining why systemic IR does not result in GI (**Figure 1H**).

Taken together, human and mouse data show that infection transiently induces IR, but does not result in overt GI due to compensatory hyperinsulinemia.

Viral infection enhances progression of diabetes mellitus type 2 in obesity

Systemic IR is the underlying cause of DM2. However, people are only diagnosed as diabetics when systemic IR has reached a level at which compensatory mechanisms fail to lower blood glucose concentrations below well-defined threshold. Thus, DM2 is diagnosed by measuring GI, rather than IR. In pre-diabetes, frequently an unknown “event” drives rapid development of DM2 (Tabak et al., 2012). To see whether infection represents such an event, animals were placed on a diet with high fat-content (HFD), resulting in diet-induced obesity (DIO). HFD generates systemic IR and GI in three months (Wensveen et al., 2015a), but after 6 weeks results only in hepatic IR, characterized by increased FPG and pyruvate intolerance (**Figure S1C, D**), but not yet systemic IR or GI (**Figure S1E, F**), thus resembling human pre-

diabetes (Mason et al., 2007). Infection of 6 weeks HFD-primed (`pre-diabetic`) mice with MCMV resulted in both IR and GI (**Figure 1I, J**), but did not affect obesity (**Figure S1G**). To test whether other viral pathogens also affect glucose homeostasis, we infected pre-diabetic mice with lymphocytic choriomeningitis (LCMV) or Influenza A virus. Both infections resulted in similar loss of glucose control as observed after MCMV infection (**Figure S1H, I**).

An important question from the perspective of clinical relevance is whether the impact of infection on glycemic control is transient or permanent. Indeed, we observed that three weeks after MCMV infection, pre-diabetic mice still showed increased GI (**Figure 1K**) although there was no difference in viral titers between normal chow diet (NCD) or HFD fed animals (**Figure S1J**), suggesting a long-lasting effect. When MCMV infection and HFD feeding were started on the same day, increased IR and reduced glycemic control were observed for at least 8 weeks in infected animals, compared to non-infected controls (**Figure 1L, M)**. In contrast, the impact of Influenza A or LCMV infection on glucose intolerance of HFD-primed animals appeared to be transient (**Figure S1K, L**).

Chronic uncontrolled DM2 is associated with development of microvascular and macrovascular complications, such as diabetic nephropathy (DN). To investigate whether infection aggravates development of DM2-associated complications, animals were infected with MCMV on the same day when we started with HFD feeding. At 16 weeks, infection of pre-diabetic mice promoted hypertrophy of juxtamedullary glomeruli, an early sign of DN (Shahbazian and Rezaii, 2013) (**Figure 1N**). After 24 weeks, histological analysis revealed more severe symptoms of DN in 10-20% of glomeruli of infected HFD-fed mice, but not in lean or uninfected animals, whereas kidneys from obese mice were mildly affected in only 5% of glomeruli (**Figure 1O; S1M**). 24 weeks after infection, viral replication was not detectible in kidneys of mice fed either with NCD or HFD, indicating that virus-induced pathology is not directly responsible for DN (**Figure S1N**). In addition, infection with MCMV in HFD fed animals resulted in increased thickness of the basement membrane, another bona fide marker of DN (**Figure 1P**).

Our findings indicate that viral infection is an independent risk factor for development of diabetes by pre-diabetic obese individuals. To investigate whether we could therapeutically prevent GI in pre-diabetic mice, animals were treated with the antiviral drug ganciclovir starting one day after infection. Ganciclovir treatment strongly reduced viral replication

(**Figure S1O**) and prevented development of virus-induced glucose intolerance in HFD primed mice (**Figure 1Q**).

In summary, viral infection of "pre-diabetic" obese mice cause a reduction of glycemic control and aggravates development of clinical symptoms associated with DM2.

Viral infection promotes development of glucose intolerance and insulin resistance through interferon-γ

To gain insight in the mechanism underlying virus-induced progression of DM2 we first investigated whether viral infection affects glucose sensing by the pancreas after HFD priming. We observed that infection of pre-diabetic mice with MCMV resulted in increased FPI and enhanced insulin production following glucose challenge (**Figure 2A**). To further prove that MCMV infection increases insulin secretion we calculated the insulinogenic index, which positively correlates with insulin output from pancreatic β-cells (Dalmas et al., 2017). We observed that the insulinogenic index was increased in infected, HFD-fed animals compared to controls, excluding pancreatic dysfunction as a cause for GI (**Figure 2B**).

The liver has an important role in maintaining euglycemia through gluconeogenesis, glycogenolysis and glycogenesis. Liver diseases, including viral hepatitis, are therefore frequently associated with aberrations in glucose homeostasis (Barthel and Schmoll, 2003; Cotrozzi et al., 1997; Custro et al., 2001; Holstein et al., 2002; Picardi et al., 2006; Postic et al., 2004; Tappy and Minehira, 2001). To investigate whether liver damage alone may be responsible for enhanced progression of GI in our model, pre-diabetic mice were exposed to the hepatotoxic compounds CCL_4 (Boll et al., 2001) or paracetamol (Mossanen and Tacke, 2015) (**Figure S2A, B**). Neither compound induced development of GI in pre-diabetic animals (**Figure S2C, D**).

We therefore considered the possibility that the immune system drives IR through specific cytokines following infection. Viral infection activates the inflammasome (Lamkanfi and Dixit, 2014), which generates the pro-diabetic cytokine IL-1β (Ballak et al., 2015). However, neither chemical inhibition of the NLRP3 inflammasome activity, nor neutralization of IL-1β with antibodies resulted in amelioration of GI following MCMV infection of pre-diabetic mice (**Figure S2E, F**). In fact, neutralization of IL-1β increased glucose intolerance following infection, which corresponds with the previously reported positive effect of this

cytokine on glycemic control (Dror et al., 2017). Type-1 inflammatory cytokines such as interferons and TNF, have a negative impact on glucose homeostasis in the context of obesity (Fensterl and Sen, 2009; Grzelkowska-Kowalczyk and Wieteska-Skrzeczynska, 2009; Kim and Solomon, 2010; Koivisto et al., 1989; McGillicuddy et al., 2009; Nieto-Vazquez et al., 2008; Wada et al., 2011; Yki-Jarvinen et al., 1989). We therefore injected lean and pre-diabetic mice with Poly I: C, a strong inducer of type-1 interferons (Wu et al., 2014). Whereas this treatment did activate peritoneal macrophages, no impact on GI was observed (**Figure S2G, H**). TNF has been shown to induce IR in *ob/ob* mice through TNF receptor 1 (TNFR1) (Uysal et al., 1998). However, deficiency for TNFR1 did not result in amelioration of GI following MCMV infection of pre-diabetic animals (**Figure S2I**). In contrast, although neutralization of interferon-γ (IFN-γ) was associated with increased viral titers in some tissues important for glucose homeostasis (**Figure S2J**), neutralization of IFN-γ completely prevented GI and IR in MCMV and LCMV infected pre-diabetic animals (**Figure 2C, D; S2K**). Similar results were achieved in *Ifng*$^{-/-}$ mice (**Figure S2L**). This data shows that IFN-γ plays a dominant role in progression of DM2 induced by different viruses.

IFN-γ is produced exclusively by immune cells (Schroder et al., 2004) following viral infection, in particular by NK cells, CD4^{+} and CD8^{+} T cells. We depleted NK, CD4^{+} or CD8^{+} T cells in MCMV infected, pre-diabetic mice (**Figure 2E, F**). Only elimination of NK cells resulted in a loss of GI (**Figure 2F**). To investigate whether NK cells have a prolonged effect on glycemic control in obese animals, we infected NK cell-depleted mice simultaneously with the start of HFD. Depletion of NK cells completely prevented development of GI 8 weeks after infection (**Figure S2M**). To confirm that NK cells drive GI through IFNγ, *Ifng*$^{-/-}$ mice received PBS or WT NK cells preceding MCMV infection. Only in the presence of WT NK cells, did *Ifng*$^{-/-}$mice develop IR (**Figure 2G**). In addition, infection of HFD primed mice with m157-deficient MCMV virus (Δ*m157*), which precludes Ly49h-mediated activation of NK cells, did not induce development of GI (**Figure S2N**). Thus, MCMV infection drives development of GI and IR in pre-diabetic mice via NK cell-derived IFN-γ.

In summary, virally-induced IFN-γ promotes IR and GI and drives the rapid progression from pre-diabetes to DM2 in infected mice.

Interferon-γ specifically induces insulin resistance of skeletal muscle cells

To investigate whether systemic or local increase of IFN-γ concentrations is responsible for the effect, pre-diabetic mice were infected with MCMV and plasma IFN-γ concentrations were followed over time. We observed that increased blood IFN-γ returned to baseline at time points when it still impacted GI and IR (**Figure 3A**). This result suggests that IFN-γ either has a long-lasting effect on the ability of tissues to sense insulin, or that there is a local source of IFN-γ which sustains impairment of insulin sensitivity. We neutralized IFN-γ starting 7 days post infection (p.i.) of HFD primed mice, when its concentrations in the blood have returned to baseline. GI was completely prevented in treated mice (**Figure 3B**), which indicates that a local source of IFN-γ drove continued GI and IR in pre-diabetic mice following infection.

Previously we showed that NK cell derived IFN-γ promotes IR in the DIO model by inducing M1 adipose tissue macrophage (ATM) polarization (Wensveen et al., 2015a). We hypothesized that this mechanism also operates in the context of infection. Whereas infection does enhance ATM conversion and tissue inflammation, clodronate-mediated neutralization of these cells did not prevent infection-induced GI (**Figure S3A, B**). To confirm that IFN-γ mediates its effect in infected mice independently of macrophages, we conditionally ablated the receptor for IFN-γ (IFNγR1) on these cells. *Lyz2*^{cre}*Ifngr1*$^{flox/flox}$ (*Ifngr1*$^{\Delta Mac}$) and littermate controls were placed on HFD for 6 weeks and then infected with MCMV. Five days p.i. we observed no difference in insulin sensitivity (**Figure 3C**) or GI (**Figure 3D)** between *Ifngr1*$^{\Delta Mac}$ and littermate controls. Thus, IFN-γ mediates its effect on IR and GI in infected pre-diabetic mice independently of macrophages.

We therefore considered that IFN-γ directly affects insulin sensitivity of one or more organs involved in glucose homeostasis. In the DIO model, VAT is the main source of chronic systemic inflammation and plays a key role in the development of IR and GI. We have shown previously that surgical removal of VAT (VATectomy) prevents development of GI and IR in non-infected obese mice (Wensveen et al., 2015a). We performed VATectomy two weeks before initiation of HFD feeding and MCMV infection. GTT was performed ten weeks after the surgery. As expected, VATectomy reduced glucose intolerance in non-infected animals. In contrast, removal of visceral fat pads was not able to prevent infection-induced GI (**Figure 3E**). Since VATectomy does not remove all adipocyte deposits in mice, we conditionally ablated IFNγR1 on adipocytes. Pre-diabetic *Adipoq*^{cre} *Ifngr1*$^{flox/flox}$ mice (*Ifngr1*$^{\Delta Adi}$) were not

able to prevent infection-induced IR or GI in comparison to littermate controls (**Figure 3F, G**). Thus, adipocytes do not play a major role in infection-induced GI in pre-diabetic mice.

To investigate whether infection reduces insulin sensitivity of the liver, pre-diabetic mice were infected with MCMV. One-week p.i. we observed that DIO, but not infection increased FPG concentrations (**Figure 3H**). In addition, one-week p.i. we analyzed gluconeogenesis by pyruvate tolerance test (PTT). In line with FPG concentrations, we observed that HFD increased gluconeogenesis following pyruvate challenge. However, infection did not result in enhanced, but even in somewhat reduced gluconeogenesis (**Figure 3I**). In addition, hepatocytes from HFD-fed mice showed reduced induction of AKT phosphorylation (pAKT) in response to insulin challenge compared to NCD-fed mice, whereas infection did not further impair this process (**Figure 3J**). Finally, hepatocyte-specific ablation of the IFNγR1 using *Alb*^{cre}*Ifngr1*$^{flox/flox}$ animals (*Ifngr1*$^{\Delta Hep}$) did not result in a reduction of IR or GI following infection of pre-diabetic mice (**Figure S3C**). To confirm that infection does not result in hepatic insulin resistance, we calculated endogenous glucose production rate (EGP) under basal conditions and after infusion of insulin during hyperinsulinemic-euglycemic clamp study. We did not observe an impact of infection on EGP under either condition (**Figure 3K**). Thus, infection-induced IR and GI is mediated independently of macrophages, adipocytes and hepatocytes.

Next, we considered skeletal muscle as a target tissue. Skeletal muscle is responsible for 70-75% of insulin-induced glucose absorption (DeFronzo et al., 1981; Shulman et al., 1990). We noticed that infection, but not DIO increases IFN-γ transcription in skeletal muscle seven days post infection (**Figure S4**). Therefore, we hypothesized that infection directly targets insulin sensitivity of muscle cells. Indeed, we observed that infection reduced pAKT in muscle of lean and obese animals upon insulin challenge (**Figure 4A**). This effect was IFN-γ-dependent, since we did not observe this effect in *Ifng*$^{-/-}$ mice (**Figure 4B**). Moreover, *Ckm*^{cre}*Ifngr1*$^{flox/flox}$ mice (*Ifngr1*$^{\Delta Myo}$), which lack the IFNγR1 receptor on myocytes, were protected from infection-induced IR and GI (**Figure 4C**). To demonstrate that infection specifically impairs glucose uptake into skeletal muscle in response to insulin, mice were subjected to hyperinsulinemic-euglycemic clamping and were injected with a bolus of radioactive 2-deoxy glucose at the end of the steady state period. We noted that glucose uptake in muscle was strongly reduced following infection, whereas internalization in VAT was not affected (**Figure 4D**).

These results demonstrate that skeletal muscle cells are the main targets of IFN-γ induced IR and progression of DM2 following infection.

Interferon-γ drives insulin resistance of skeletal muscle cells through downregulation of the insulin receptor

Next, we sought to elucidate how infection-induced IFN-γ drives IR in muscle. Infection did not affect total Akt protein expression, suggesting that IFN-γ impairs upstream insulin receptor signaling. No differences were observed in transcription of *Irs1* and *Irs2* (**Figure S5A**). Also, we found no increase in *Socs1* or *Socs3*, which are known targets of IFN-γ and known inhibitors of insulin signaling (Wormald et al., 2006) (**Figure S5B**). In contrast, transcription of *Insr*, coding for the insulin receptor, was significantly reduced in muscle, but not in liver of infected pre-diabetic mice (**Figure 5A**). Moreover, we found that infection of WT, but not *Ifng*$^{-/-}$mice with MCMV resulted in downregulation of insulin receptor expression on transcriptional and protein amounts in muscle (**Figure 5B-D; S5C, D)**. Likewise, infection with LCMV or Influenza A also resulted in down-regulation of *Insr* in muscle (**Figure S5E**). To investigate whether IFN-γ alone induces downregulation of *Insr* or whether this effect is only achieved in the context of viral infection, we injected IFN-γ daily in the *m. sartorius* of NCD or HFD primed mice. We observed that IFN-γ injection alone was able to cause upregulation of MHC II, a bona fide downstream target of IFNγR signaling, on muscle tissue macrophages (**Figure S5F**) and downregulation of *Insr* transcript in muscle but not in the liver (**Figure 5E, S5G**).

Since MCMV infection has a long lasting negative effect on insulin sensitivity, at least in pre-diabetic mice, we wanted to elucidate whether 3 weeks p.i. *Insr* is still downregulated in muscle. We observed that transcription of *Insr* in muscle of HFD primed MCMV infected mice are still down-regulated at this time point (**Figure 5F**).

Taken together, these results suggest that infection-induced IFN-γ drives IR in skeletal muscles through downregulation of the insulin receptor, resulting in GI in pre-diabetic animals.

Infection-induced insulin resistance promotes antiviral CD8$^+$ T cell responses

Finally, we questioned the physiological relevance of IFN-γ-induced IR. In lean animals, infection did not induce hyperglycemia, excluding increased nutrient availability as a cause. However, viral infection did cause hyperinsulinemia. Since insulin receptor and CD28 signaling both converge on PI3K (Frauwirth et al., 2002), we hypothesized that insulin may directly provide co-stimulation for CD8$^+$ T cells. We observed that CD8$^+$ T cells expressed both *Insr* and *Irs2,* but not *Irs1* (**Figure 6A**). Indeed, stimulation of primed CD8$^+$ T cells with insulin rapidly induced phosphorylation of S6 kinase (**Figure 6B**), a downstream target of insulin-signaling. Next, we stimulated OT-1 CD8$^+$ T cells in vitro with SIINFEKL peptides and/or αCD28 antibodies in the presence or absence of insulin. Proliferation and viability were not affected by insulin (**Figure S6A, B**). In contrast, cytokine and Granzyme B production were enhanced by insulin, especially upon CD28 co-stimulation (**Figure 6C**).

To confirm these findings *in vivo* in an obesity-independent model of hyperinsulinemia, lean mice were injected daily with basal (long-acting) insulin. Unlike short-working insulin used in ITT, basal insulin was slowly released in the blood stream and caused a continuous state of hyperinsulinemia. Basal insulin-treated animals were infected with MCMV and CD8$^+$ T cell responses were analyzed after seven days. We observed that hyperinsulinemia promoted effector cell formation and cytokine production of virus-specific CD8$^+$ T cells (**Figure 7A, B**).

To test the importance of insulin on CD8$^+$ T cell priming in a second model, we generated *Ins2*^{cre} iDTR mice which allow elimination of insulin-producing pancreatic beta cells by injection of diphtheria toxin (DT). DT-treatment of *Ins2*^{cre} iDTR abrogated their ability to produce insulin in response to a glucose bolus (**Figure S7A, B, C**), but did not result in overt morbidity at least one week after treatment. DT-treated *Ins2*^{cre} iDTR or iDTR littermates were infected with MCMV and CD8$^+$ T cell responses were analyzed one week later. DT-treatment caused reduction in the number of virus-specific CD8$^+$ T cells upon MCMV infection and impaired their cytokine production (**Figure 7C, D**). Finally, after MCMV infection, DT-treated *Ins2*^{cre} iDTR mice had reduced capacity to kill viral peptide-pulsed target cells (**Figure 7E**). To confirm that virus-induced muscle IR was responsible for the enhanced CD8$^+$ T cell response we infected *Ifngr1*$^{\Delta Myo}$ mice and littermate controls with MCMV and analyzed CD8$^+$ T cell responses one week later. Prevention of skeletal muscle IR caused reduction in the number KLRG1$^+$ virus-specific CD8$^+$ T cells (**Figure 7F**). Moreover, CD8$^+$ T cells showed impaired

cytokine production upon in vitro re-stimulation (**Figure 7G**). Thus, we have identified insulin as a molecule which promotes antiviral-effector $CD8^+$ T cell responses.

DISCUSSION

Our research has addressed the question how viral infection contributes to development of DM2. We found that the activated immune system drove systemic IR in response to infection with various viruses, but not GI due to compensatory insulin output by the pancreas. In case of pre-existing metabolic dysfunction caused by DIO, compensatory mechanisms were overloaded and long-term loss of glycemic control ensued. We discovered that virally-induced IFN-γ directly and specifically targeted skeletal muscle to downregulate the insulin receptor and promoted compensatory hyperinsulinemia to boost the $CD8^+$ T cell-mediated antiviral immune response. Thus, here we have identified a physiological feed-back mechanism between the immune and endocrine systems which operates in viral infection and we demonstrate that this mechanism represents an "Achilles heel" for deregulation of glycemic control in pre-diabetic obese subjects.

Current opinion in the field holds that IR is a derailed physiological response to systemic inflammation that aims to increase the systemic glucose set point to ensure optimal nutrient availability for activated immune cells (Kotas and Medzhitov, 2015). Indeed, extreme conditions, such as severe trauma or sepsis are able to induce hyperglycemia (Dungan et al., 2009). Chronic injection of high-doses of LPS, a mouse model for severe sepsis (Doi et al., 2009), is shown to induce hepatic insulin resistance and increase FPG through modification of the mevalonate pathway (Okin and Medzhitov, 2016). However, this so-called stress hyperglycaemia is only observed in critically ill patients (Dungan et al., 2009), and not following common infections such as we have investigated. Activated $CD8^+$ T cells dramatically increase their requirement for glucose to satisfy needs for growth, proliferation and effector function (Maciver et al., 2008). Nevertheless, glucose uptake rather than glucose availability has shown to be the rate limiting step for effector $CD8^+$ T cell function (Jacobs et al., 2008). Indeed, even at glucose concentrations that were tenfold lower than those normally observed during homeostasis, maximal $CD8^+$ T cell effector function was achieved in the presence of sufficient co-stimulation (Jacobs et al., 2008). This seems at odds with the observation that starvation promotes lethality upon influenza infection of mice, which could be prevented by oral glucose gavage (Wang et al., 2016). However, caloric supplementation

during viral infection does not induce loss of glycemic control (Wang et al., 2016). Our findings suggest that glucose administration during infection promotes immune responses indirectly by increasing systemic insulin concentrations. Indeed, when we abrogated insulin production in mice, we observed reduced $CD8^+$ T cell responsiveness, despite a state of systemic hyperglycemia.

CD28 provides one of the strongest co-stimulatory signals for activation of $CD8^+$ T cells through the activation of several signaling cascades, including the PI3K pathway (Rudd et al., 2009). The insulin receptor exclusively signals through PI3K, thus sharing a major signaling cascade with CD28. Indeed, we found that insulin stimulation of $CD8^+$ T cells during priming enhanced the costimulatory effects of CD28 and functioned as a pro-inflammatory cytokine. Immune cell-mediated increase of insulin availability at the time of $CD8^+$ T cells priming, therefore benefits the immune response. However, immune-mediated adjustment of insulin production comes at a risk of inducing loss of glucose homeostasis and should therefore be carefully regulated. For example, if IFN-γ would directly stimulate pancreatic insulin production, it would induce potentially lethal hypoglycemia. Similarly, induction of IR in liver or VAT would result in an increase of FPG or circulating free fatty acids respectively (Karpe et al., 2011; Leto and Saltiel, 2012; Meshkani and Adeli, 2009). By targeting insulin sensitivity of muscle, increased insulin production by the pancreas both boosts the antiviral immune response, whilst ensuring blood glucose homeostasis. Muscle IR could cause reduced motility, but this is in fact a desirable behavior upon infection (Wang et al., 2016). Recently, it has been shown that under homeostatic conditions macrophage-derived IL-1β can promote insulin secretion which stimulates glucose uptake in immune cells (Dror et al., 2017). Our findings indicate that IL-1β does not reduce systemic glucose uptake following infection. However, neutralization of IL-1β resulted in enhanced glucose intolerance following infection, suggesting that immune-endocrine interactions operate at multiple levels to increase systemic insulin concentration.

The role of obesity-induced visceral adipose tissue inflammation in development of IR has been well described. Adipocyte hypertrophy promotes accumulation of pro-inflammatory cells with a Th1 cell-signature, such as $CD8^+$ T cells and M1 macrophages. Cytokines such as TNF, IL-6 and IL-1β produced by these cells leak into circulation and induce insulin resistance (Johnson et al., 2012). We and others have shown that NK cell derived IFN-γ promotes development of IR indirectly by driving conversion of adipose tissue macrophages (ATMs)

towards an M1 phenotype (O'Rourke et al., 2012; Wensveen et al., 2015a). Infection-induced IR appears to operate independently of VAT. Moreover, we have demonstrated *in vivo* that IFN-γ is able to induce IR directly in non-immune cells. *In vitro*, IFN-γ had been shown to cause IR in 3T3-L1 adipocytes and myoblast by inhibiting insulin receptor signaling through induction of suppressor of cytokine signaling (SOCS) molecules (Grzelkowska-Kowalczyk and Wieteska-Skrzeczynska, 2009; McGillicuddy et al., 2009; Wada et al., 2011). We show that *in vivo* IFN-γ specifically reduced glucose uptake in skeletal muscle by downregulation of the insulin receptor.

DM2 affects almost half a billion of people worldwide with tens of millions more at risk of developing this disease (American Diabetes, 2018). In this study we showed that viral infection was a hyperglycemia-inducing "event" that was able to drive rapid transition from pre-diabetes to diabetes. Infectious diseases such as cytomegalovirus and influenza, for which we show that they cause IR in humans and mice, affect most of the human population (Colugnati et al., 2007). Prospective studies show that IR develops years to decades before onset of DM2. Increased β cell output of insulin compensates IR, resulting only in a marginal increase of FPG and 2HG (Tabak et al., 2009). When insulin resistance reaches a level that cannot be compensated anymore by increased insulin production of the pancreas, blood glucose values rapidly rise and DM2 ensues. We found that infection-induced IR was able to push animals beyond this threshold. However, the metabolic state of the subject (i.e. is hepatic IR established), as well as the nature and intensity of the infection appear to be crucial for determining whether the effect of the infection will be transient or permanent. Our results therefore have direct implications for the way health care specialists should approach infections or vaccination strategies in patients with pre-diabetes, since prevention of DM2 might be most effective at the time of this transition (Mason et al., 2007). Our findings indicate that, in addition to well established criteria such as obesity, hypertension and high triglyceride concentrations in circulation, viral infection should be considered as an important risk factor for development of DM2, especially in patients with prediabetes (American Diabetes, 2018).

Author contributions

M.Š. designed and carried out most of the experiments and analyzed data. S.M. and I.K. performed and analyzed some experiments. I.B. generated key research reagents. Đ.C. and T.T.W. were involved in human study. S.J. was involved in some experiments designed. S.W. and D.K. designed and performed clamp studies. F.M.W and B.P. directed the research and wrote the paper with M.Š., with input from all coauthors.

Acknowledgements

We thank to B. Trošelj-Vukić, I. Pavić and L. Bilić-Zulle for their support to the clincal part of the study, A. Waisman for generous help with iDTR mice and M. Golemac for histochemistry. We also thank to S. Slavić-Stupac, D. Rumora, K. Miklić, S. Malić, M. Samsa, E. Ražić, E. Marinović and A. Miše for excellent technical assistance and animal care. This work was supported by the University of Rijeka (865.10.2101 to FMW and 803.10.1103 to BP), the Croatian Science Foundation (IP-2016-06-8027 to FMW and IP-2016-06-9306 to BP), the European Social Fund for Croatia (HR.3.2.01-0263 to BP), the Unity through Knowledge Fund (UKF 15/13 to BP), and the grant KK.01.1.1.01.0006, awarded to the Scientific Centre of Excellence for Virus Immunology and Vaccines and co-financed by the European Regional Development Fund to SJ. This work was also supported by grants from the Swiss National Science Foundation (#310030-179344 to DK).

Declaration of Interests

The authors declare no competing interests.

REFERENCES

Abdul-Ghani, M.A., Tripathy, D., and DeFronzo, R.A. (2006). Contributions of beta-cell dysfunction and insulin resistance to the pathogenesis of impaired glucose tolerance and impaired fasting glucose. Diabetes Care *29*, 1130-1139.

American Diabetes, A. (2018). 2. Classification and Diagnosis of Diabetes: Standards of Medical Care in Diabetes-2018. Diabetes Care *41*, S13-S27.

Ballak, D.B., Stienstra, R., Tack, C.J., Dinarello, C.A., and van Diepen, J.A. (2015). IL-1 family members in the pathogenesis and treatment of metabolic disease: Focus on adipose tissue inflammation and insulin resistance. Cytokine *75*, 280-290.

Barthel, A., and Schmoll, D. (2003). Novel concepts in insulin regulation of hepatic gluconeogenesis. American journal of physiology. Endocrinology and metabolism *285*, E685-692.

Boll, M., Weber, L.W., Becker, E., and Stampfl, A. (2001). Mechanism of carbon tetrachloride-induced hepatotoxicity. Hepatocellular damage by reactive carbon tetrachloride metabolites. Zeitschrift fur Naturforschung. C, Journal of biosciences *56*, 649-659.

Chen, S., de Craen, A.J., Raz, Y., Derhovanessian, E., Vossen, A.C., Westendorp, R.G., Pawelec, G., and Maier, A.B. (2012). Cytomegalovirus seropositivity is associated with glucose regulation in the oldest old. Results from the Leiden 85-plus Study. Immun Ageing *9*, 18.

Colugnati, F.A., Staras, S.A., Dollard, S.C., and Cannon, M.J. (2007). Incidence of cytomegalovirus infection among the general population and pregnant women in the United States. BMC infectious diseases *7*, 71.

Cotrozzi, G., Casini Raggi, V., Relli, P., and Buzzelli, G. (1997). [Role of the liver in the regulation of glucose metabolism in diabetes and chronic liver disease]. Annali italiani di medicina interna : organo ufficiale della Societa italiana di medicina interna *12*, 84-91.

Custro, N., Carroccio, A., Ganci, A., Scafidi, V., Campagna, P., Di Prima, L., and Montalto, G. (2001). Glycemic homeostasis in chronic viral hepatitis and liver cirrhosis. Diabetes & metabolism *27*, 476-481.

Dalmas, E., Lehmann, F.M., Dror, E., Wueest, S., Thienel, C., Borsigova, M., Stawiski, M., Traunecker, E., Lucchini, F.C., Dapito, D.H.*, et al.* (2017). Interleukin-33-Activated Islet-Resident Innate Lymphoid Cells Promote Insulin Secretion through Myeloid Cell Retinoic Acid Production. Immunity *47*, 928-942 e927.

Defronzo, R.A. (2009). Banting Lecture. From the triumvirate to the ominous octet: a new paradigm for the treatment of type 2 diabetes mellitus. Diabetes *58*, 773-795.

DeFronzo, R.A., Ferrannini, E., Sato, Y., Felig, P., and Wahren, J. (1981). Synergistic interaction between exercise and insulin on peripheral glucose uptake. The Journal of clinical investigation *68*, 1468-1474.

Doi, K., Leelahavanichkul, A., Yuen, P.S., and Star, R.A. (2009). Animal models of sepsis and sepsis-induced kidney injury. The Journal of clinical investigation *119*, 2868-2878.

Dror, E., Dalmas, E., Meier, D.T., Wueest, S., Thevenet, J., Thienel, C., Timper, K., Nordmann, T.M., Traub, S., Schulze, F.*, et al.* (2017). Postprandial macrophage-derived IL-1beta stimulates insulin, and both synergistically promote glucose disposal and inflammation. Nature immunology *18*, 283-292.

Dungan, K.M., Braithwaite, S.S., and Preiser, J.C. (2009). Stress hyperglycaemia. Lancet *373*, 1798-1807.

Durward, M., Harms, J., and Splitter, G. (2010). Antigen specific killing assay using CFSE labeled target cells. J Vis Exp.

Fensterl, V., and Sen, G.C. (2009). Interferons and viral infections. Biofactors *35*, 14-20.

Frauwirth, K.A., Riley, J.L., Harris, M.H., Parry, R.V., Rathmell, J.C., Plas, D.R., Elstrom, R.L., June, C.H., and Thompson, C.B. (2002). The CD28 signaling pathway regulates glucose metabolism. Immunity *16*, 769-777.

Ganeshan, K., and Chawla, A. (2014). Metabolic regulation of immune responses. Annu Rev Immunol *32*, 609-634.

Grzelkowska-Kowalczyk, K., and Wieteska-Skrzeczynska, W. (2009). Treatment with IFN-gamma prevents insulin-dependent PKB, p70S6k phosphorylation and protein synthesis in mouse C2C12 myogenic cells. Cell Biol Int *34*, 117-124.

Heinrich, P.C., Behrmann, I., Haan, S., Hermanns, H.M., Muller-Newen, G., and Schaper, F. (2003). Principles of interleukin (IL)-6-type cytokine signalling and its regulation. The Biochemical journal *374*, 1-20.

Hirche, C., Frenz, T., Haas, S.F., Doring, M., Borst, K., Tegtmeyer, P.K., Brizic, I., Jordan, S., Keyser, K., Chhatbar, C.*, et al.* (2017). Systemic Virus Infections Differentially Modulate Cell Cycle State and Functionality of Long-Term Hematopoietic Stem Cells In Vivo. Cell Rep *19*, 2345-2356.

Holstein, A., Hinze, S., Thiessen, E., Plaschke, A., and Egberts, E.H. (2002). Clinical implications of hepatogenous diabetes in liver cirrhosis. Journal of gastroenterology and hepatology *17*, 677-681.

Jacobs, S.R., Herman, C.E., Maciver, N.J., Wofford, J.A., Wieman, H.L., Hammen, J.J., and Rathmell, J.C. (2008). Glucose uptake is limiting in T cell activation and requires CD28-mediated Akt-dependent and independent pathways. J Immunol *180*, 4476-4486.

Johnson, A.R., Milner, J.J., and Makowski, L. (2012). The inflammation highway: metabolism accelerates inflammatory traffic in obesity. Immunol Rev *249*, 218-238.

Karpe, F., Dickmann, J.R., and Frayn, K.N. (2011). Fatty acids, obesity, and insulin resistance: time for a reevaluation. Diabetes *60*, 2441-2449.

Kim, S.Y., and Solomon, D.H. (2010). Tumor necrosis factor blockade and the risk of viral infection. Nat Rev Rheumatol *6*, 165-174.

Koivisto, V.A., Pelkonen, R., and Cantell, K. (1989). Effect of interferon on glucose tolerance and insulin sensitivity. Diabetes *38*, 641-647.

Kotas, M.E., and Medzhitov, R. (2015). Homeostasis, inflammation, and disease susceptibility. Cell *160*, 816-827.

Krmpotic, A., Bubic, I., Polic, B., Lucin, P., and Jonjic, S. (2003). Pathogenesis of murine cytomegalovirus infection. Microbes Infect *5*, 1263-1277.

Lamkanfi, M., and Dixit, V.M. (2014). Mechanisms and functions of inflammasomes. Cell *157*, 1013-1022.

Leinonen, M., and Saikku, P. (1999). Interaction of Chlamydia pneumoniae infection with other risk factors of atherosclerosis. Am Heart J *138*, S504-506.

Leto, D., and Saltiel, A.R. (2012). Regulation of glucose transport by insulin: traffic control of GLUT4. Nature reviews. Molecular cell biology *13*, 383-396.

Maciver, N.J., Jacobs, S.R., Wieman, H.L., Wofford, J.A., Coloff, J.L., and Rathmell, J.C. (2008). Glucose metabolism in lymphocytes is a regulated process with significant effects on immune cell function and survival. Journal of leukocyte biology *84*, 949-957.

Marik, P.E., and Raghavan, M. (2004). Stress-hyperglycemia, insulin and immunomodulation in sepsis. Intensive Care Med *30*, 748-756.

Mason, C.C., Hanson, R.L., and Knowler, W.C. (2007). Progression to type 2 diabetes characterized by moderate then rapid glucose increases. Diabetes *56*, 2054-2061.

Matthews, D.R., Hosker, J.P., Rudenski, A.S., Naylor, B.A., Treacher, D.F., and Turner, R.C. (1985). Homeostasis model assessment: insulin resistance and beta-cell function from fasting plasma glucose and insulin concentrations in man. Diabetologia *28*, 412-419.

McGillicuddy, F.C., Chiquoine, E.H., Hinkle, C.C., Kim, R.J., Shah, R., Roche, H.M., Smyth, E.M., and Reilly, M.P. (2009). Interferon gamma attenuates insulin signaling, lipid storage, and differentiation in human adipocytes via activation of the JAK/STAT pathway. J Biol Chem *284*, 31936-31944.

Meshkani, R., and Adeli, K. (2009). Hepatic insulin resistance, metabolic syndrome and cardiovascular disease. Clinical biochemistry *42*, 1331-1346.

Mossanen, J.C., and Tacke, F. (2015). Acetaminophen-induced acute liver injury in mice. Laboratory animals *49*, 30-36.

Munzberg, H., and Morrison, C.D. (2015). Structure, production and signaling of leptin. Metabolism *64*, 13-23.

Nieto-Vazquez, I., Fernandez-Veledo, S., Kramer, D.K., Vila-Bedmar, R., Garcia-Guerra, L., and Lorenzo, M. (2008). Insulin resistance associated to obesity: the link TNF-alpha. Arch Physiol Biochem *114*, 183-194.

O'Neill, L.A., Kishton, R.J., and Rathmell, J. (2016). A guide to immunometabolism for immunologists. Nat Rev Immunol *16*, 553-565.

O'Rourke, R.W., White, A.E., Metcalf, M.D., Winters, B.R., Diggs, B.S., Zhu, X., and Marks, D.L. (2012). Systemic inflammation and insulin sensitivity in obese IFN-gamma knockout mice. Metabolism: clinical and experimental *61*, 1152-1161.

Okin, D., and Medzhitov, R. (2016). The Effect of Sustained Inflammation on Hepatic Mevalonate Pathway Results in Hyperglycemia. Cell *165*, 343-356.

Ouchi, N., Parker, J.L., Lugus, J.J., and Walsh, K. (2011). Adipokines in inflammation and metabolic disease. Nat Rev Immunol *11*, 85-97.

Pessin, J.E., and Saltiel, A.R. (2000). Signaling pathways in insulin action: molecular targets of insulin resistance. The Journal of clinical investigation *106*, 165-169.

Picardi, A., D'Avola, D., Gentilucci, U.V., Galati, G., Fiori, E., Spataro, S., and Afeltra, A. (2006). Diabetes in chronic liver disease: from old concepts to new evidence. Diabetes/metabolism research and reviews *22*, 274-283.

Postic, C., Dentin, R., and Girard, J. (2004). Role of the liver in the control of carbohydrate and lipid homeostasis. Diabetes & metabolism *30*, 398-408.

Roberts, B.W., and Cech, I. (2005). Association of type 2 diabetes mellitus and seroprevalence for cytomegalovirus. South Med J *98*, 686-692.

Rudd, C.E., Taylor, A., and Schneider, H. (2009). CD28 and CTLA-4 coreceptor expression and signal transduction. Immunol Rev *229*, 12-26.

Schroder, K., Hertzog, P.J., Ravasi, T., and Hume, D.A. (2004). Interferon-gamma: an overview of signals, mechanisms and functions. Journal of leukocyte biology *75*, 163-189.

Shahbazian, H., and Rezaii, I. (2013). Diabetic kidney disease; review of the current knowledge. Journal of renal injury prevention *2*, 73-80.

Sharpe, A.H., and Freeman, G.J. (2002). The B7-CD28 superfamily. Nat Rev Immunol *2*, 116-126.
Shulman, G.I., Rothman, D.L., Jue, T., Stein, P., DeFronzo, R.A., and Shulman, R.G. (1990).

Quantitation of muscle glycogen synthesis in normal subjects and subjects with non-insulin-dependent diabetes by 13C nuclear magnetic resonance spectroscopy. The New England journal of medicine *322*, 223-228.

Stevens, G.A., Singh, G.M., Lu, Y., Danaei, G., Lin, J.K., Finucane, M.M., Bahalim, A.N., McIntire, R.K., Gutierrez, H.R., Cowan, M.*, et al.* (2012). National, regional, and global trends in adult overweight and obesity prevalences. Popul Health Metr *10*, 22.

Tabak, A.G., Herder, C., Rathmann, W., Brunner, E.J., and Kivimaki, M. (2012). Prediabetes: a high-risk state for diabetes development. Lancet *379*, 2279-2290.

Tabak, A.G., Jokela, M., Akbaraly, T.N., Brunner, E.J., Kivimaki, M., and Witte, D.R. (2009). Trajectories of glycaemia, insulin sensitivity, and insulin secretion before diagnosis of type 2 diabetes: an analysis from the Whitehall II study. Lancet *373*, 2215-2221.

Tappy, L., and Minehira, K. (2001). New data and new concepts on the role of the liver in glucose homeostasis. Current opinion in clinical nutrition and metabolic care *4*, 273-277.

Uysal, K.T., Wiesbrock, S.M., and Hotamisligil, G.S. (1998). Functional analysis of tumor necrosis factor (TNF) receptors in TNF-alpha-mediated insulin resistance in genetic obesity. Endocrinology *139*, 4832-4838.

Wada, T., Hoshino, M., Kimura, Y., Ojima, M., Nakano, T., Koya, D., Tsuneki, H., and Sasaoka, T. (2011). Both type I and II IFN induce insulin resistance by inducing different isoforms of SOCS expression in 3T3-L1 adipocytes. American journal of physiology. Endocrinology and metabolism *300*, E1112-1123.

Wagner, F.M., Brizic, I., Prager, A., Trsan, T., Arapovic, M., Lemmermann, N.A., Podlech, J., Reddehase, M.J., Lemnitzer, F., Bosse, J.B.*, et al.* (2013). The viral chemokine MCK-2 of murine cytomegalovirus promotes infection as part of a gH/gL/MCK-2 complex. PLoS Pathog *9*, e1003493.

Wang, A., Huen, S.C., Luan, H.H., Yu, S., Zhang, C., Gallezot, J.D., Booth, C.J., and Medzhitov, R. (2016). Opposing Effects of Fasting Metabolism on Tissue Tolerance in Bacterial and Viral Inflammation. Cell *166*, 1512-1525 e1512.

Wensveen, F.M., Jelencic, V., Valentic, S., Sestan, M., Wensveen, T.T., Theurich, S., Glasner, A., Mendrila, D., Stimac, D., Wunderlich, F.T.*, et al.* (2015a). NK cells link obesity-induced adipose stress to inflammation and insulin resistance. Nat Immunol *16*, 376-385.

Wensveen, F.M., Valentic, S., Sestan, M., Wensveen, T.T., and Polic, B. (2015b). The "Big Bang" in obese fat: events initiating obesity-induced adipose tissue inflammation. Eur J Immunol.

Wormald, S., Zhang, J.G., Krebs, D.L., Mielke, L.A., Silver, J., Alexander, W.S., Speed, T.P., Nicola, N.A., and Hilton, D.J. (2006). The comparative roles of suppressor of cytokine signaling-1 and -3 in the inhibition and desensitization of cytokine signaling. J Biol Chem *281*, 11135-11143.

Wu, J., Huang, S., Zhao, X., Chen, M., Lin, Y., Xia, Y., Sun, C., Yang, X., Wang, J., Guo, Y.*, et al.* (2014). Poly(I:C) treatment leads to interferon-dependent clearance of hepatitis B virus in a hydrodynamic injection mouse model. Journal of virology *88*, 10421-10431.

Wueest, S., Rapold, R.A., Schumann, D.M., Rytka, J.M., Schildknecht, A., Nov, O., Chervonsky, A.V., Rudich, A., Schoenle, E.J., Donath, M.Y., and Konrad, D. (2010). Deletion of Fas in adipocytes relieves adipose tissue inflammation and hepatic manifestations of obesity in mice. The Journal of clinical investigation *120*, 191-202.

Yki-Jarvinen, H., Sammalkorpi, K., Koivisto, V.A., and Nikkila, E.A. (1989). Severity, duration, and mechanisms of insulin resistance during acute infections. The Journal of clinical endocrinology and metabolism *69*, 317-323.

Figure 1. Viral infection induces IR, but GI only after HFD-priming. Patients with respiratory infection were segregated in two groups (normal weight: BMI <25 (n=17), overweight: BMI>25 (n=14)) and analyzed at time of diagnosis and after 3 months for (**A**) FPI (**B**) FPG and (**C**) HOMA-IR index. (**D**) MCMV titters (PFU) in indicated tissues of B6 mice at day 4, 7 and 10 p.i. are shown. LD=limit of detection. (**E**) B6 mice were mock-infected or infected with MCMV and analyzed 7 days later by ITT. (**F**) B6 mice were mock-infected or infected with MCMV and analyzed 5 days later by hyperinsulinemic-euglycemic clamp. Glucose infusion rate (GIR) is shown. n=5. (**G-H**) B6 mice were mock-infected or infected with MCMV and analyzed 7 days later by (**G**) GTT and (**H**) serum insulin concentrations after glucose challenge upon overnight fasting were measured. In addition, area under curve is shown. (**I-K**) Mice were placed on NCD or HFD for 6 weeks ('pre-diabetic' mice) before infection with MCMV or PBS. One week later, they were subjected to (**I**) ITT or (**J**) GTT. (**K**) GTT was also performed three weeks after infection. (**L-P**) Mice were infected with MCMV simultaneously with the start of HFD. Eight weeks p.i. mice were subjected to (**L**) GTT and (**M**) ITT. In addition, (**N**), sizes of juxtamedullary glomeruli were determined 16 weeks p.i. (n=5; 72 glomeruli per animal). 24 weeks p.i. (**O**) PAS staining of kidney sections was performed. (Green arrow) expansion of mesangial matrix and (yellow arrow) increased Bowman capsule size or (**P**) thickness of basement membrane are shown. (**Q**) MCMV infected pre-diabetic mice were treated daily with ganciclovir starting 24 h p.i. or with PBS. After seven days, mice were subjected to GTT. The experiment in Figure F was performed once. For all other experiments, a representative of three experiments is shown. For (**D-Q**) five mice were used in each group. Indicated are means ± s.e.m. and statistical significances at * $p<0.05$, ** $p<0.01$, ***$p<0,001$ by (**A-C, E-H)** Student`s t test or (**I-Q**) ANOVA followed by Bonferroni post-testing. p.i. - post infection. See also Figure S1.

Figure 2. Infection-induced IFN-γ promotes development of GI and IR in pre-diabetic mice. (**A-F**) Mice were fed for 6 weeks with indicated diets, followed by MCMV infection. Control mice were treated with PBS. (**A**) Seven days p.i., mice were fasted overnight and challenged with glucose. Insulin concentartions were determined in serum by ELISA. (**B**) Insulinogenic index during GTT. (**C, D**) Infected pre-diabetic or NCD-fed mice were injected every three days with neutralizing mAbs to IFN-γ or with isotype matched irrelevant mAbs starting 24 h before infection. (**C**) GTT and (**D**) ITT were performed on day 7 after infection. Infected pre-diabetic mice injected with (**E**) CD4- or CD8-depleting, or (**F**) NK cell depleting antibodies. Control animals were treated with isotype matched irrelevant mAbs. GTT was performed on day 7 p.i.. (**G**) B6 or *Ifng*$^{-/-}$ mice were infected with MCMV. *Ifng*$^{-/-}$ mice were transferred with NK cells or PBS one day before infection and three days later. Five days p.i. mice were subjected to ITT. For (**A-G**) representative of three experiments is shown. For (**A-G**) five mice were used in each group. Indicated are means ± s.e.m. and statistical significances at * $p<0.05$, ** $p<0.01$, ***$p<0,001$ by ANOVA followed by Bonferroni post-testing. p.i. - post infection. See also Figure S2.

Figure 3. Infection-induced IR and GI is mediated independently of macrophages, adipocytes and hepatocytes. (**A**) Serum IFN-γ concentrations were determined by ELISA at different time points after infection of mice primed with HFD or NCD for 6 weeks. (**B**) Pre-diabetic mice were MCMV or mock infected and treated with neutralizing mAbs to IFN-γ every three days starting one day before or 7 days p.i. Fourteen days p.i. mice were subjected to GTT. (**C, D**) Pre-diabetic *Ifngr1*$^{\Delta Mac}$ mice and *Ifngr1*$^{lox/flox}$ littermates were injected with MCMV or PBS. Seven days p.i. mice were subjected to (**C**) ITT or (**D**) GTT. (**E**) Mice either underwent sham operation or surgical excision of periepididymal fat pad (VATectomy). Two weeks after surgery, mice were infected with MCMV and placed on HFD. GTT was performed after 8 weeks. (**F, G**) Pre-diabetic *Ifngr1*^{Adi} mice and *Ifngr1*$^{flox/flox}$ littermates were injected with MCMV or PBS. Five and seven days after infection mice were subjected to (**F**) ITT or (**G**) GTT respectively. (**H-J**) Mice were fed for 6 weeks with indicated diets, followed by MCMV or PBS injection. (**H**) FPG was determined seven days after infection. (**I**) PTT was performed on day seven after infection. **(J**) Seven days p.i., mice were fasted overnight, followed by injection with insulin. After 30 minutes liver samples were isolated and pan-Akt and pAkt amounts were determined by Immuno blotting. (**K**) B6 mice were mock-infected or infected with MCMV and endogenous glucose production was analyzed 5 days later during hyper-insulinemic-euglycemic clamp. **(H)** Pooled data of 12 experiments (n=60) is shown (analyzed by ANOVA with Bonferroni post-testing). The experiment in **Figure 3K** was performed once. Other graphs show one of two or more experiments with similar results. For (**A-G**) and (**I-K**) five mice were used in each group. Indicated are means ± s.e.m. and statistical significances at * $p<0.05$, ** $p<0.01$, ***$p<0,001$ by student`s t test or ANOVA followed by Bonferroni post-testing. p.i. - post infection. See also Figure S3.

Figure 4. IFN-γ induces IR specifically in the skeletal muscle. (**A, B**) B6 and *Ifng*$^{-/-}$ mice were NCD or HFD-fed for 6 weeks, followed by MCMV infection. After seven days mice were fasted overnight, followed by injection with insulin. After 30 minutes skeletal muscle samples were isolated and pan-Akt and pAkt amounts were determined by Immuno blotting. (**C**) Pre-diabetic *Ifngr1*^{Myo} mice and *Ifngr1*$^{lox/flox}$ littermates were injected with MCMV or PBS. Five and seven days p.i., mice were subjected to ITT and GTT. (**D**) Glucose uptake into VAT and skeletal muscle during hyperinsulinemic-euglycemic clamping 5 days after MCMV infection of NCD fed mice. The experiment in Figure D was performed once. In (**A, B**) density quantification plot shows pooled data from two independent experiments. For C a representative of three experiments is shown. For (**A-D**) five mice per experiment were used in each group. Indicated are means ± s.e.m. and statistical significances at * $p<0.05$, ** $p<0.01$, ***$p<0,001$ by (**D**) Student`s t test or (**A-C**) ANOVA followed by Bonferroni post-testing. p.i. - post infection. See also Figure S4.

Figure 5. IFNγ induces IR in the skeletal muscle through downregulation of the insulin receptor. (**A**) Pre-diabetic or NCD fed mice were infected with MCMV or left untreated. On day 7 after infection, *Insr* transcripts were determined in muscle and liver by qPCR. Expression was normalized to *Hprt*. (**B**) Skeletal muscle samples were isolated 7 days after MCMV infection of pre-diabetic mice, and protein expression of insulin receptor was determined by immuno blot. (**C, D**) *Ifng*$^{-/-}$ mice were MCMV or mock infected and after five days skeletal muscle samples were isolated and (**C**) *Insr* expression was determined by qPCR. Expression was normalized to *Hprt*. (**D**) Protein expression of the InsR were determined by Immuno blot. (**E**) Pre-diabetic or NCD fed mice were injected daily in one *m. sartorius* with mouse recombinant IFN-γ or PBS. After 3 days, transcript of *Insr* were determined in *m. sartorius*. R (right)- site of injection; L (left) – collateral symmetric muscle. (**F**) Prediabetic or NCD fed mice were infected with MCMV. Three weeks p.i. *Insr* expression in muscle was determined by qPCR. Representative of two (**E, F**) or three (**A-D**) experiments is shown. For (**A-F**) at least four mice were used in each group. Indicated are means ± s.e.m. and statistical significances at * $p<0.05$, ** $p<0.01$, ***$p<0,001$ by (**A, E-F**) ANOVA followed by Bonferroni post-testing or (**B-D**) Student`s t test. p.i. - post infection. See also Figure S5. InsR – protein expression.

Figure 6. Insulin promotes activation of CD8$^+$ T cells (**A**) qPCR was used to quantify expression of *Insr*, *Irs2* and *Irs1* in purified OT-1 CD8$^+$ T cells. Expression was normalized to *Hprt*. (**B**) Purified OT-1 cells were stimulated with SIINFEKL (N4) peptide in the presence or absence of anti-CD28. After 2 days, cells were rested from stimuli for 3h, followed by stimulation with 1 IU/ml of insulin. Kinetics of S6 phosphorylation were determined by flow cytometry. Representative plot shows cells primed with N4 and αCD28 at 0 and 15min after insulin stimulation. (**C**) Purified OT-1 cells were stimulated with N4 peptide alone or in the presence of insulin and/or anti-CD28. After 48 h, cells were re-stimulated with N4 peptide and production of Granzyme B, IFN-γ and TNF was measured by flow cytometry. For (**A-C**) a representative of at least three experiments is shown. For (**A**-**C**) at least three samples were used in each group Indicated are means ± s.e.m. and statistical significances at * $p<0.05$, ** $p<0.01$, ***$p<0,001$ by (**C**) ANOVA followed by Bonferroni post-testing. See also Figure S6.

Fig. 7. Insulin promotes anti-viral CD8$^+$ effector T cell responses. (**A, B**) B6 mice were infected with MCMV and treated daily with basal insulin or PBS. Seven days p.i. (**A**) effector cells (KLRG1$^+$) specific for two MCMV epitopes were quantified in spleen. Histograms show representative plots. Gated on CD8$^+$ tetramer$^+$ cells. (**B**) Splenocytes were re-stimulated in vitro with indicated peptides and TNF production was analyzed by flow cytometry. (**C-E**) *Ins2*^{cre}Rosa^{iDTR} and Rosa^{iDTR} littermates were DT-treated and subsequently infected with MCMV. After seven days (**C**) absolute numbers of antigen-specific cells were determined in spleen. (**D**) Splenocytes were re-stimulated *in vitro* with viral peptides and cytokine production was analyzed by flow cytometry. (**E**) Mice were injected with splenocytes pulsed with control, m57 or m139 peptides, labelled with different CFSE concentrations. After 4h, specific killing was determined in spleen. (**F, G**) *Ifngr1*^{Myo} mice and *Ifngr1*$^{flox/flox}$ littermates were infected with MCMV. After seven days (**F**) effector cells (KLRG1$^+$) specific for two MCMV epitopes were quantified in spleen. In addition, (**G**) splenocytes were re-stimulated in vitro with two different viral peptides and production of the IFN-γ and TNF was analyzed with flow cytometry. For (**A-E**) five mice and for (**F-G**) eight mice were used in each group. Representative of two or more experiments is shown. Indicated are means ± s.e.m. and statistical significances at * $p<0.05$, ** $p<0.01$, ***$p<0,001$ by (**A-G**) Student`s t test. p.i. - post infection. See also Figure S7.

STAR METHODS

CONTACT FOR REAGENT AND RESOURCE SHARING

As Lead Contact, BP is responsible for all reagent and resource requests. Please contact BP at bojan.polic@medri.uniri.hr with requests and inquiries.

EXPERIMENTAL MODEL AND SUBJECT DETAILS

Mouse strains

Male mice were strictly age- and sex-matched within experiments and handled in accordance with institutional and national guidelines. All mice were housed and bred under specific pathogen free condition at the animal facility of the Medical faculty, University of Rijeka. Wild type C57BL/6J (B6; strain 664), *Ifng*$^{-/-}$ (2287), *Ifngr1*$^{flox/flox}$ (25394), *Adipoq*^{cre} (10803), *Ckm*^{cre} (6475), *Ins2*^{cre} (003573), *Alb*^{cre} (003574), *Lyz2*^{cre} (4781), B6 Ly5.1 (2014) and OT-1 (3831) mice were obtained from the Jackson Laboratory. iDTR were a kind gift from prof. Ari Waisman, Mainz, Germany. All genetically modified animal models were generated on the C57BL/6J background or backcrossed at least ten times with C57BL/6J mice. Male mice (8-12 weeks old) were fed *ad libitum* either with NCD (SSNIFF) or with HFD in which 50% of calories was derived from animal fat (Bregi). All animal experiments were approved by the National Committee for welfare of animals.

Viruses

The bacterial artificial chromosome–derived murine cytomegalovirus (BAC-MCMV) strain pSM3fr-MCK-2fl clone 3.3 has previously been shown to be biologically equivalent to the MCMV Smith strain (VR-1399; ATCC) and is referred to as wild-type (WT) MCMV (Wagner et al., 2013). pSM3fr-MCK-2fl clone 3.3 and Δ*m157* (Hirche et al., 2017) were propagated on mouse embryonic fibroblasts (MEF). Animals were infected intravenously i.v. with $2x10^5$ PFU. Viral titers were determined on MEF by standard plaque assay. Lymphocytic choriomeningitis virus (LCMV) Armstrong strain (Armstrong E-350; ATCC) was propagated on baby mouse kidney cells according to standard protocol. Animals were infected intraperitoneally i.p. with 10^6 PFU. Influenza A strain A/PR/8/34 (ATCC) was generated in LLC-MK2 cells and $TCID_{50}$ was determined in wild-type B6 mice. Mice were infected intranasally with 10 x $TCID_{50}$ under ketamine/xylazine anesthesia.

Glucose tolerance, insulin tolerance and pyruvate tolerance test

For glucose tolerance (GTT) and insulin tolerance (ITT) tests mice were fasted for 6 h and then injected with 1g/kg of D-glucose (Sigma) i.p. or with 1 U/kg of human fast working insulin (Aspart, Novo Nordisk) dissolved in saline solution, respectively. In the end of ITT mice were injected i.p. with 1 g/kg of D-glucose (Sigma) to prevent consequence of the hypoglycemia. To measure pyruvate tolerance (PTT), mice were fasted for 16 h and then injected with 1 g/kg i.p. of pyruvate sodium solution (Sigma). Glucose was measured in blood from the *v. saphena* with an automated glucometer (SD Codefree). ITT is a standard metabolic test that is commonly used to assess sensitivity of the insulin receptor before and after insulin administration, while GTT measures glucose disposal after glucose challenge. These two tests are commonly used to detect impairments in glucose metabolism.

Insulinogenic index

To investigate the impact of the infection on insulin secretion we calculated insulinogenic index. Insulinogenic index is defined as a ratio between insulin areas and glucose areas under curve during GTT (Dalmas et al., 2017).

Glucose clamp studies

Hyperinsulinemic-euglycemic clamp studies were performed in freely moving mice as described (Wueest et al., 2010). Mice were anesthetized with isofluran and eye ointment was applied to both eyes. A catheter (MRE 025, Braintree Scientific, Braintree, MA, USA) was inserted into the left jugular vein and exteriorized at the neck. Two to three days after surgery, DMEM (control) or $2x10^5$ PFU MCMV virus dissolved in DMEM was injected via catheter. Five days p.i., hyperinsulinemic-euglycemic clamp was performed. Insulin was infused at a constant rate (12 mU/kg*min) and steady state glucose infusion rate was calculated once glucose infusion reached a more or less constant rate for 15-20 min with blood glucose concentrations at 5-6 mmol/l. The glucose disposal rate was calculated by dividing the rate of [3-3H] glucose infusion by the plasma [3-3H] glucose specific activity. Endogenous glucose production during the clamp was calculated by subtracting the glucose infusion rate from the glucose disposal rate. In order to assess tissue specific glucose uptake, a bolus (10 μCi) of 2-[1-14C] deoxyglucose was administered via catheter at the end of the steady state period. Blood

was sampled 2, 15, 25 and 35 min after bolus delivery. Area under the curve of disappearing plasma 2-[1-14C] deoxyglucose was used together with tissue-concentration of phosphorylated 2-[1-14C] deoxyglucose to calculate glucose uptake.

ELISA

To analyze serum insulin concentrations, animals were fasted overnight and injected with 1 g/kg of D-glucose. Blood was isolated from the *v. saphena* using heparin coated plastics. Insulin was measured in plasma using the mouse ultrasensitive insulin ELISA kit (Alpco). IFN-γ concentrations were measured with the mouse IFN-gamma Platinum ELISA (eBioscience) according to manufacturer`s protocol. Plates were analyzed using a Mithras LB940 ELISA plate reader (Berthold technologies).

ImmunoBlot

After overnight fasting, mice were injected with 1 U/kg of human fast working insulin (Aspart, Novo Nordisk). After 30 min VAT, liver and muscle were isolated and snap-frozen in liquid nitrogen. Samples were lysed in Triton lysis buffer (50 mM HEPES, 1% Triton X-100, 10 mM EDTA, 0.1% SDS, 50 mM NaCl, complete ULTRA Tablets, Mini, Easypack (Protease inhibitor cocktail tablets) (Roche) and PhosStop EASYpack (Phosphatase inhibitor cocktail tablets) (Roche) in a tissue homogenizer. Protein contents were determined by the Pierce BCA Protein Assay Kit (Thermo Fisher Scientific) and equal amounts of total lysate were analyzed by 12% SDS-polyacrylamide gel electrophoresis. Proteins were transferred to Immobilon-P and incubated with blocking buffer (Tris buffered saline/Tween-20) containing 2% low-fat milk for 1 h before incubating with an antibody against the insulin receptor, p-Akt (Ser^{473}) and pan-Akt from Cell Signaling. Bands were visualized with ECL Prime Immuno Blotting Detection Reagent (GE Healthcare) using ImageQuant LAS 4000mini (GE Healthcare, Life Science). Density of bands was calculated relative to pan-Akt using ImageJ software.

Quantitative PCR

Muscle (*m. sartorius*) or liver pieces were lysed in Trizol with a tissue homogenizer. RNA was isolated via the Trizol method (Invitrogen), and cDNA was generated with a reverse

transcriptase core kit (Eurogentec). The expression of mRNA was examined by quantitative PCR with a 7500 Fast Real Time PCR machine (ABI). Taqman assays were used to quantify the expression of *Ifng* (Mm00485148_m1) and *Socs3* (Mm00545913_s1). The relative mRNA expression was normalized by quantification of *β-actin* (*Actb,* Mm00607939_s1) RNA in each sample. For expression of *Insr*, *Socs1*, *Irs1* and *Irs2* qPCR was performed by monitoring in real time the increase in fluorescence of the SYBR Green dye (Eurogentec) according to manufacturer`s protocol. Primer sequences were as follows: *Insr* forward 5′-TTTGTCATGGATGGAGGCTA-3′ and reverse 5′ CCTCATCTTGGGGTTGAACT-3', *Socs1* forward 5'- GATTCTGCGTGCCGCTCT-3' and reverse 5'-TGCGTGCTACCATCCTACTC-3', *Irs1* forward 5'- CTCTACACCCGAGACGAACAC-3' and reverse 5'- TGGGCCTTTGCCCGATTATG-3', *Irs2* forward 5'-CGAGTCAATAGCGGAGACCC-3' and reverse 5'- CCCCTGAGACCCTACGGTAA-3'.The relative mRNA expression was normalized by quantification of *Hrts (forward 5'-* CACAGGACTAGAACACCTGC-3' and reverse 5'- GCTGGTGAAAAGGACCTCT-3').

Antibodies and Flow cytometry

Antibodies for *in vivo* applications (CD4 (YTS191.1.2), CD8 (YTS169.4.2), NK1.1 (PK136), IFN-γ (R4-6A2), Il-1β (BE0246) and isotype controls were produced by our in-house facility or purchased from BioXcell. For flow cytometry, single-cell suspensions of spleen were prepared according to standard protocols. Flow cytometric analysis were performed by using anti-mouse mouse CD4 (GK1.5), CD3 (145-2C11), CD8β (53-6.7), CD62L (MEL-14), CD127 (A7R34), KLRG1 (2F1), NK1.1 (PK136), CD11b (M1/70), CD11c (N418), CD86 (GL1), GR1 (RB6 8C5), F4/80 (BM8), TNF (MP6-XT22), IFN-γ (XMG1.2) and granzyme B (NGZB) from eBioscience, preceded by blocking of Fc receptors using 2.4G2 antibodies (in house generated). To measure cytokine production, cells were stimulated with 1 μg of MCMV peptides M57 (SCLEFWQRV) or m139 (TVYGFCLL) or with SIINFEKL (N4) peptide for 4 h in the presence of Brefeldin A (10 μg/ml; eBioscience). MHC class I tetramers were provided by A. ten Brinke (Amsterdam, The Netherlands). For intracellular staining, permeabilization and fixation of cells was done with the Fix/Perm kit (BD Biosciences). All data were acquired using a FACSVerse (BD Biosciences) and analyzed using FlowJo software (Tree Star).

Human data

Patients in the age group of 18-70yrs, diagnosed with acute respiratory infection (Influenza, Human respiratory syncytial virus (HRSV)) were recruited from the Dept. of Infectology at the Clinical Medical Center of Rijeka. Pneumonia was diagnosed with chest x-ray. Influenza and HRSV were determined by PCR on RNA isolated from nasopharyngeal swabs by our clinical diagnostics laboratory. Patients suffering from kidney failure, chronic inflammatory or autoimmune diseases or patients with a previous history of glucose intolerance or diabetes (anamnesis and HbA1c) were excluded from this study. Whole blood was drawn on two-time points: acute infection (days 1-7 from the onset of symptoms) and post illness period (90-100 days after first analysis). Insulin concentrations were measured in plasma by electro-chemiluminescence immunoassay (ECLIA) on a Cobas E411 analyzator (Roche, Switzerland) and HbA1c were measured in full blood using a turbidimetric inhibition immunoassay (TINIA) on a Cobas 501 analyzator (Roche, Switzerland). Body mass index of every patient was determined at first analysis. Fasting insulin and glucose concentrations were used to calculate HOMA-IR as described (Matthews et al., 1985) . An informed consent was obtained from patients after the nature and possible consequences of the studies were explained. This study was approved by the University of Rijeka Medical Faculty Ethics Committee before initiation.

Methods performed *in vivo*

VATectomy was done as described (Wensveen et al., 2015a). In brief, mice either underwent sham operation or had periepididymal fat pad removed (VATectomy). Two weeks after surgery, mice were placed on NCD or HFD and infected with MCMV or left untreated. For adoptive transfer, NK cells were isolated and purified using biotinylated DX5 antibodies, streptavidin-coated beads and magnetic cell sorting (Miltenyi) from spleen and blood. Purity was determined by flow cytometry. $5x10^6$ NK cells were transferred i.v. in to *Ifng*$^{-/-}$ mice one day before infection and three days after initial transfer. For induction of liver damage using CCL_4, mice were treated twice a week with 200 µl of a 10% solution of CCL_4 diluted in mineral oil. To induce liver damage with paracetamol, animals received 100 mg/kg of paracetamol dissolved in PBS twice per week. For depletion of macrophages, mice were injected once weekly with 45 mg/kg of clodronate liposomes or with unloaded liposomes as a control starting one day before infection. Poly I:C was injected i.p. twice per week at 200 µg per mouse.

MCC950 (Cayman Chemical) was administrated i.p. every second day at doses of 20 mg/kg. Poly I:C and MCC950 treatments were started one day before infection with MCMV. For depletion of pancreatic β-cells in Ins2^{cre}iDTR mice, 25 ng/g of Diphteria Toxin (DT, Merck) was injected i.p. 48 h and 24 h before infection. Hyperinsulinemia in mice was achieved with daily i.p. injection of 10 IU/kg of basal insulin (Degludek, Novo Nordisk), starting one day before infection with MCMV. For inhibition of viral replication, mice were injected i.p. once daily, starting one day post infection, with 40 mg/kg of ganciclovir (MCE), diluted in PBS. 10^4 UI of mouse recombinant IFN-γ was injected daily in to m. sartorius. In vivo killer assay was done as described (Durward et al., 2010). Briefly, DT-treated Ins2^{cre}iDTR and iDTR littermate controls were infected with MCMV. After seven days animals were injected i.v. with $5x10^6$ CD45.1 splenocytes. Before transfer splenocytes were pulsed for 1 h with 1 μg/ml M57 (MCMV), M139 (MCMV) or PB1-F2 (Flu) peptides, washed and mixed in 1:1:1 ratio. Cells could be distinguished based on differential CFSE (Molecular Probes) labeling. 4 h after transfer, specific killing of MCMV-pulsed cells, relative to Flu-pulsed cells was determined in spleen using flow cytometry.

Cell assays

CD8$^+$ OT-1 T cells were purified by magnetic cell separation (Miltenyi, Biotec). Cells were cultured in RPMI 1640 medium (PAN-Biotech), supplemented with 10% FCS (PAN-Biotech) and 2-ME (Sigma-Aldrich). Cells were CFSE-labeled and stimulated in vitro with 1 ng/ml of SIINFEKL (N4) peptide in presence or absence of 0.5 μg/ml of αCD28 (37.51, eBioscience) and 1 U/ml of insulin (Aspart, Novo Nordisk). For proliferation, CFSE dilution was determined by flow cytometry after 72 h. For cytokine production, after 48 h of culture, cells were re-stimulated with 10 ng/ml N4 peptide in presence of Brefeldin A. After 4 h cytokines were measured by intracellular flow cytometry. For phosphorylation kinetics of S6, cells were stimulated with ng/ml N4 peptide in the presence or absence of 0.5 μg/ml of αCD28. After 2 days, cells were stimulated with 1 U/ml of fast working insulin insulin (Aspart, Novo Nordisk) for 0, 5, 15 and 30 min. Cells were fixed with 2% paraformaldehyde, permeabilized in 90% methanol, stained for pS6 (Cell signaling), visualized with anti-rabbit PE (eBioscience) and measured by flow cytometry.

Histology

Organs were fixed in 10% neutral buffered formalin and embedded in paraffin. For morphometric and pathohistological analyzes of kidney (glomeruli) section were stained with PAS. For PAS staining, the samples were incubated in 0.1% periodic acid for 10 min. The kidney sections were washed in running tap water for 1 min and immersed in Schiff's reagent for 17 min. Subsequently, the sections were washed in tap water for 3 min, counterstained with Mayer's hematoxylin for 2 min, washed in tap water for 3 min, and dehydrated in two changes of 96% alcohol. Finally, the sections were cleared in xylene and mounted with Entellan (Sigma Aldrich). Glomerular area was determined using the Cell^ B Soft Imaging System (Olympus). Three slides per animal and 24 glomeruli per each slide were analyzed. Analysis of diabetic nephropathy was performed on PAS-stained slides by a trained pathologist on blinded sections. For detection of liver fibrosis, liver sections were stained with Sirius red staining. First slides were baked at 60°C for 1 h and then taken through xylene and graded ethanols (100%, 95%, 85%, 75%, 60%, 50%) into distilled water. Slides were then stained overnight (minimum 14 h) in saturated picric acid with 0.1% Sirius Red F3BA (Aldrich Chemicals). The next morning slides were removed, washed in 0.01 N hydrochloric acid for 2 min, and rapidly dehydrated through graded alcohols starting at 70%, then to xylene, and finally cover slipped.

Statistical analyses

Data are presented as mean ± SEM. Statistical significance was determined by either two-tailed unpaired Student's t test, Mann Whitney (U) test or one-way ANOVA with Bonferroni correction using Graph Pad Prism 5. A value of $p>0.05$ was deemed not statistically significant (ns); *$p<0.05$, **$p<0.01$ and ***$p<0.001$.

KEY RESOURCES TABLE

REAGENT or RESOURCE	SOURCE	IDENTIFIE
Antibodies		
Rat anti mouse CD4 monoclonal antibody (clone GK1.5)	eBioscience	Cat. # 14-0041
Armenian hamster anti mouse CD3e monoclonal antibody (clone 145-2C11)	eBioscience	Cat. # 11-0031

Rat anti mouse CD11b monoclonal antibody (clone M1/70)	eBioscience	Cat. # 25-0112
Rat anti mouse CD127 monoclonal antibody (clone A7R34)	eBioscience	Cat. # 12-1271
Mouse anti mouse CD62L monoclonal antibody (clone MEL-14)	eBioscience	Cat. # 11-0621-82
Syrian hamster anti mouse KLRG1 monoclonal antibody (clone 2F1)	eBioscience	Cat. # 11-5893-82
Mouse anti mouse NK1.1 monoclonal antibody (clone PK136)	eBioscience	Cat. # 11-5941-82
Armenian hamster anti mouse CD11c monoclonal antibody (clone N418)	eBioscience	Cat. # 11-0114-82
Rat anti mouse CD86 monoclonal antibody (clone GL1)	eBioscience	Cat. # 17-0862-82
Rat anti mouse GR1 monoclonal antibody (clone RB68C5)	eBioscience	Cat. # 11-5931-82
Rat anti mouse F4/80 monoclonal antibody (clone BM8)	eBioscience	Cat. # 11-4801-82
Rat anti mouse granzyme B monoclonal antibody (clone NGZB)	eBioscience	Cat. # 11-8898-82
Rat anti mouse IFN-γ monoclonal antibody (Clone: XMG1.2)	eBioscience	Cat. # 17-7311-82
Rat anti mouse TNF monoclonal antibody (Clone: MP6-XT22)	eBioscience	Cat. # 11-7321-82
Mouse monoclonal anti-mouse β-aktin (AC-15)	Santa Cruz Biotechnology	sc-69879
Syrian hamster anti mouse CD28 (37.51) monoclonal antibody	eBioscience	Cat. # 13-0281-82
Rat anti mouse CD8β monoclonal antibody (Clone: 53-6.7)	eBioscience	Cat. # 45-0081-80
Rat IgG2a kappa Isotype control	eBioscience	Cat. # 12-4321-82
Mouse IgG1 kappa Isotype control	eBioscience	Cat. # 45-4714-80
Rat IgG2a kappa Isotype control	eBioscience	Cat. # 25-4321-81
Mouse anti mouse CD49b monoclonal antibody (biotin) (Clone: DX5)	eBioscience	Cat. # 13-5971-82
Fixable Viability Dye eFluor™ 780	eBioscience	Cat. # 65-0865-14
Rabbit anti mouse pS6 (Clone: D57.2.2)	Cell signaling	Cat. # 4858S
Rabbit anti mouse Insulin receptor (Clone: 4B8)	Cell signaling	Cat. # 3025S
Rabbit anti mouse p-Akt (Ser^{473}) (Clone: D9E)	Cell signaling	Cat. # 4060S
Rabbit anti mouse Pan-AKT (Clone:11E7)	Cell signaling	Cat. # 4685S
CD4 (Clone: YTS191.1.2)	In house produced	
CD8 (Clone: YTS169.4.2)	In house produced	
NK1.1 (Clone PK136)	BioXCell	Cat. # BP0036
IL-1β (Clone B122)	BioXCell	Cat. # BE0246

IFN-γ (Clone R4-6A2)	BioXCell	Cat. # BE0054
Mouse recombinant IFN-γ	Preprotech	Cat. # 315-05
Bacterial and Virus Strains		
MCMV strain pSM3fr-MCK-2fl clone 3.3	In-house produced	https://www.ncbi.nlm.nih.gov/pubmed/23935483
MCMV strain Δ*m157*	In-house produced	https://www.ncbi.nlm.nih.gov/pubmed/28614719
LCMV Armstrong strain (Armstrong E-350; American Type Culture Collection)	ATCC	VR-1271™
Influenza A strain A/PR/8/34	ATCC	VR-1469
Biological Samples		
N/A		
Chemicals, Peptides, and Recombinant Proteins		
Brefeldin A	eBioscience	Cat. 00-4506-51
CFSE	Sigma	CAS Number: 150347-59-4
M57, SCLEFWQRV;	Genscript	Custom
m139, TVYGFCLL;	Genscript	Custom
SIINFEKL - N4	Genscript	Custom
Poly I:C	Sigma-Aldrich	CAS Number: 42424-50-0
Glucose	Sigma-Aldrich	CAS Number: 50-99-7
2-[1-14C] deoxyglucose	PerkinElmer	NEC495A050UC
Insulin (fast working insulin)	Novo Nordisk	
Insulin (basal)	Novo Nordisk	
Pyruvate sodium solution	Sigma-Aldrich	Cas Number: 113-24-6
CCL_4	Sigma-Aldrich	CAS Number: 56-23-5
Mineral oil	Sigma-Aldrich	CAS Number: 8042-47-5

Paracetamol	Sigma-Aldrich	CAS Number: 103-90-2
MCC950	Cayman Chemical	CAS Number 210826-40-7
Diphteria Toxin	Merck	Cat. # 322326
Sirius Red F3BA	Aldrich Chemicals	CAS Number 2610-10-8
Schiff's	Sigma Aldrich	CAS Number 3952016
Mayer's hematoxylin	Sigma Aldrich	MDL Number MFCD00078111
Ganciclovir	Sigma Aldrich	CAS Number 824410-32-0
Clodronate liposomes	Liposoma	https://clodronateliposomes.com/shop/
Complete ULTRA Tablets, Mini, Easy pack (Protease inhibitor cocktail tablets)	Roche	Cat. # 05892791001
PhosStop EASYpack (Phosphatase inhibitor cocktail tablets)	Roche	Cat. # PHOSS-RO
Ketamine hydrochloride	Sigma Aldrich	CAS Number 1867-66-9
Xylazine	Sigma Aldrich	CAS Number 7361-61-7
SYBR Green dye	Eurogentec	Cat. # 05-SN2X-03T
Critical Commercial Assays		
Fixation/Permeabilization Solution Kit	BD Biosciences	Cat. # 554714
CD8a (Ly2) microbeads mouse	Miltenyi Biotec	Cat. # 130-049-401
Streptavidin MicroBeades	Miltenyi Biotec	Cat. # 130-048-101

LS columns	Miltenyi Biotec	Cat. # 130-042-401
TRIzol	Invitrogen	Cat. # 15596026
SuperScript II cDNA synthesis kit	Invitrogen	Cat. # 18064
Reverse Transcriptase Core Kit 300	Eurogentec	Cat. # 05-RTCK-03
Taqman assays *Ifng* (Mm00485148_m1)	Thermo Fisher Scientific	Cat. # 4331182
Taqman assays *Socs3* (Mm00545913_s1).	Thermo Fisher Scientific	Cat. # 4331182
Pierce BCA Protein Asay Kit	Thermo Fisher Scientific	Cat. # 23225
Mouse ultrasensitive insulin ELISA kit	Alpco	Cat. # 80-INSMSU-E01
Mouse IFN-gamma Platinum ELISA	Thermo Fisher Scientific	Cat. # BMS609
ECL Prime Western Blotting Detection Reagent	GE Healtcare	RPN2232
Catheter (MRE 025)	Braintree Scientific	MRE025 10 00 FT
Deposited Data		
N/A		
Experimental Models: Cell Lines		
N/A		
Experimental Models: Organisms/Strains		
C57BL/6 (B6; line 664)	Jackson Laboratories	JAX: 000664
Ifng$^{-/-}$	Jackson Laboratories	JAX: 00287
Ifngr1$^{flox/flox}$	Jackson Laboratories	JAX: 025394
Adipoq^{cre}	Jackson Laboratories	JAX: 010803
Ckm^{cre}	Jackson Laboratories	JAX: 006475
Ins2^{cre}	Jackson Laboratories	JAX: 003573
Alb^{cre}	Jackson Laboratories	JAX: 003574
Lyz2^{cre}	Jackson Laboratories	JAX: 004781
B6Ly5.1	Jackson Laboratories	JAX: 002014
OT-1	Jackson Laboratories	JAX: 003831

iDTR	Prof. Ari Waisman, Mainz, Germany	N/A
Primers		
Insr fwd 5′-TTTGTCATGGATGGAGGCTA-3′	Metabion	Custom
Insr rev5′ CCTCATCTTGGGGTTGAACT-3'	Metabion	Custom
Socs1 fwd 5'- GATTCTGCGTGCCGCTCT-3'	Metabion	Custom
Socs1 rev 5'- TGCGTGCTACCATCCTACTC-3'	Metabion	Custom
Irs1 fwd 5'- CTCTACACCCGAGACGAACAC-3'	Metabion	Custom
Irs1 rev 5'- TGGGCCTTTGCCCGATTATG-3	Metabion	Custom
Irs2 fwd 5'-CGAGTCAATAGCGGAGACCC-3'	Metabion	Custom
Irs2 rev 5'- CCCCTGAGACCCTACGGTAA-3	Metabion	Custom
Hprt fwd: *5'*-CACAGGACTAGAACACCTGC-3'	Metabion	Custom
Hprt rev: 5'- GCTGGTGAAAAGGACCTCT-3'	Metabion	Custom
Recombinant DNA		
N/A		
Software and Algorithms		
Flow Jo	FLOWJO, LLC (Tree Star)	
GraphPad Prism	GraphPad Software	
ImageJ	National Institutes of Health	https://imagej.nih.gov/ij/download.html
Cell^ B Soft Imaging System	Olympus	http://www.olympus-sis.com/
Other		
N/A		

Figure 1.

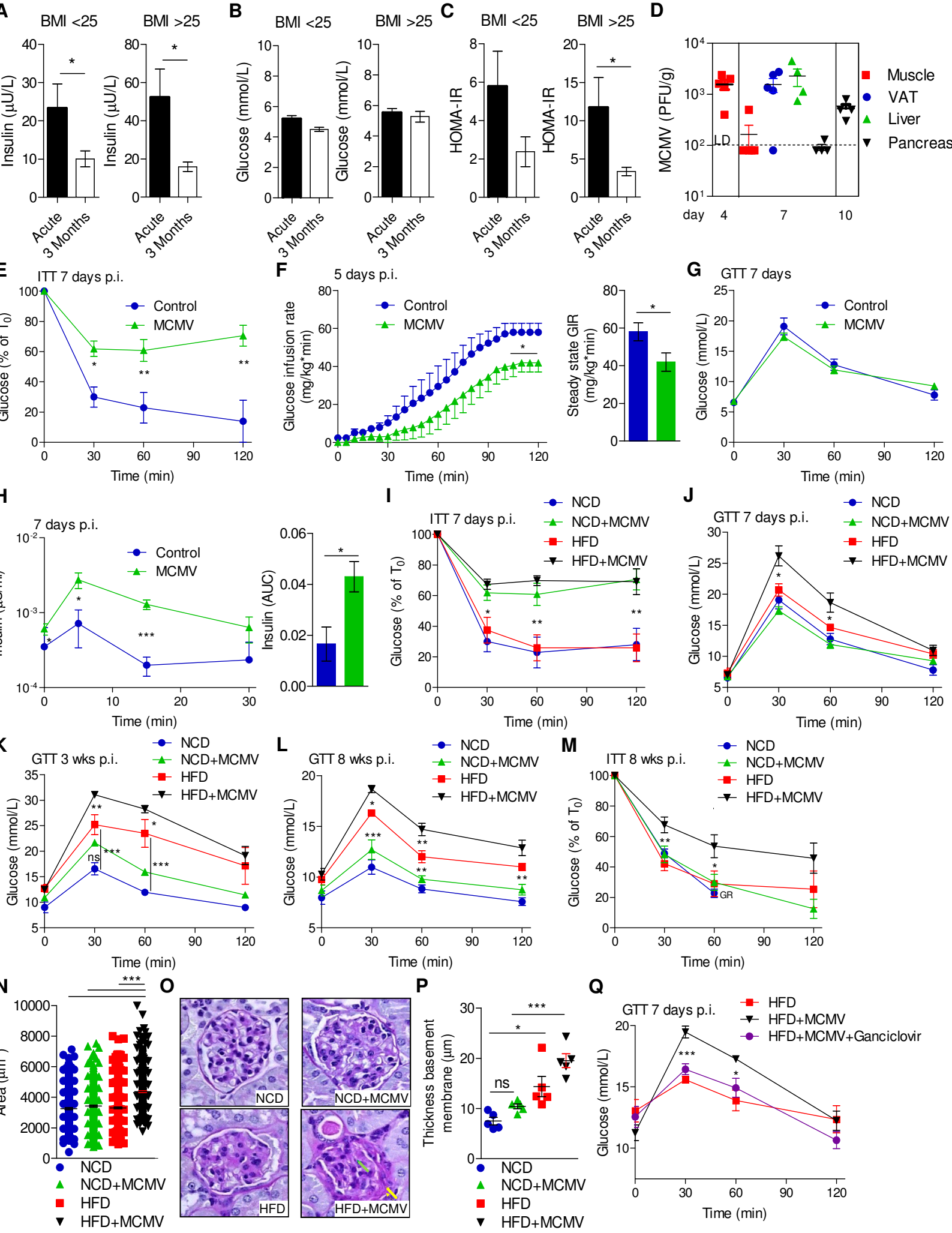
A
BMI <25
BMI >25
Insulin (µU/L)
Acute
3 Months
B
Glucose (mmol/L)
C
HOMA-IR
D
MCMV (PFU/g)
LD
day
Muscle
VAT
Liver
Pancreas
E
ITT 7 days p.i.
Control
MCMV
Glucose (% of T0)
Time (min)
F
5 days p.i.
Glucose infusion rate (mg/kg*min)
Steady state GIR (mg/kg*min)
G
GTT 7 days
H
7 days p.i.
Insulin (AUC)
I
ITT 7 days p.i.
NCD
NCD+MCMV
HFD
HFD+MCMV
J
GTT 7 days p.i.
K
GTT 3 wks p.i.
ns
L
GTT 8 wks p.i.
M
ITT 8 wks p.i.
GR
N
Area (µm²)
O
NCD
NCD+MCMV
HFD
HFD+MCMV
P
Thickness basement membrane (µm)
Q
GTT 7 days p.i.
HFD
HFD+MCMV
HFD+MCMV+Ganciclovir

Figure 2.

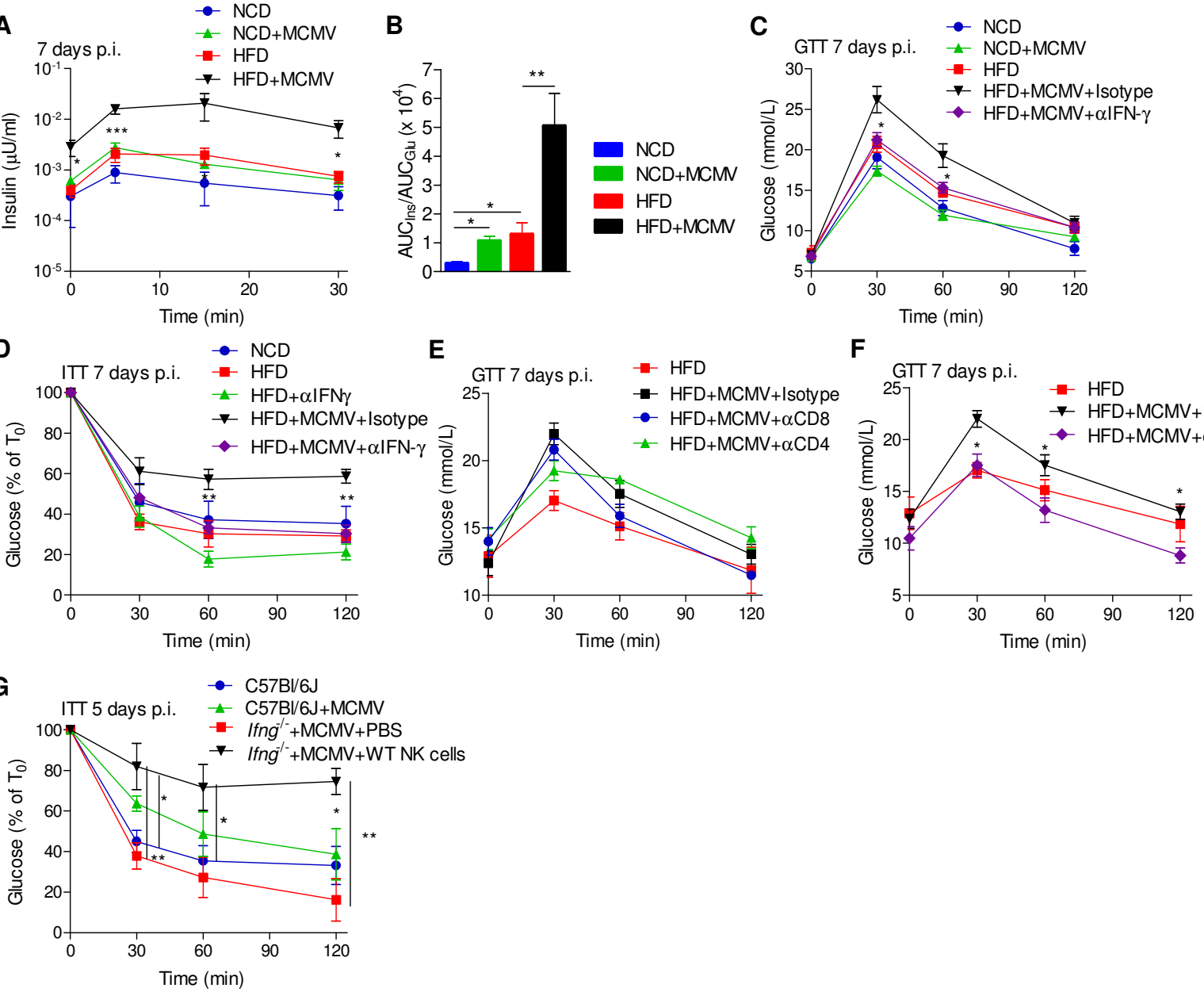
A
7 days p.i.
NCD
NCD+MCMV
HFD
HFD+MCMV
Insulin (µU/ml)
Time (min)
B
AUCIns/AUCGlu (x 10^4)
NCD
NCD+MCMV
HFD
HFD+MCMV
C
GTT 7 days p.i.
NCD
NCD+MCMV
HFD
HFD+MCMV+Isotype
HFD+MCMV+αIFN-γ
Glucose (mmol/L)
Time (min)
D
ITT 7 days p.i.
NCD
HFD
HFD+αIFNγ
HFD+MCMV+Isotype
HFD+MCMV+αIFN-γ
Glucose (% of T0)
Time (min)
E
GTT 7 days p.i.
HFD
HFD+MCMV+Isotype
HFD+MCMV+αCD8
HFD+MCMV+αCD4
Glucose (mmol/L)
Time (min)
F
GTT 7 days p.i.
HFD
HFD+MCMV+Isotype
HFD+MCMV+αNK1.
Glucose (mmol/L)
Time (min)
G
ITT 5 days p.i.
C57Bl/6J
C57Bl/6J+MCMV
Ifng-/-+MCMV+PBS
Ifng-/-+MCMV+WT NK cells
Glucose (% of T0)
Time (min)

Figure 3.

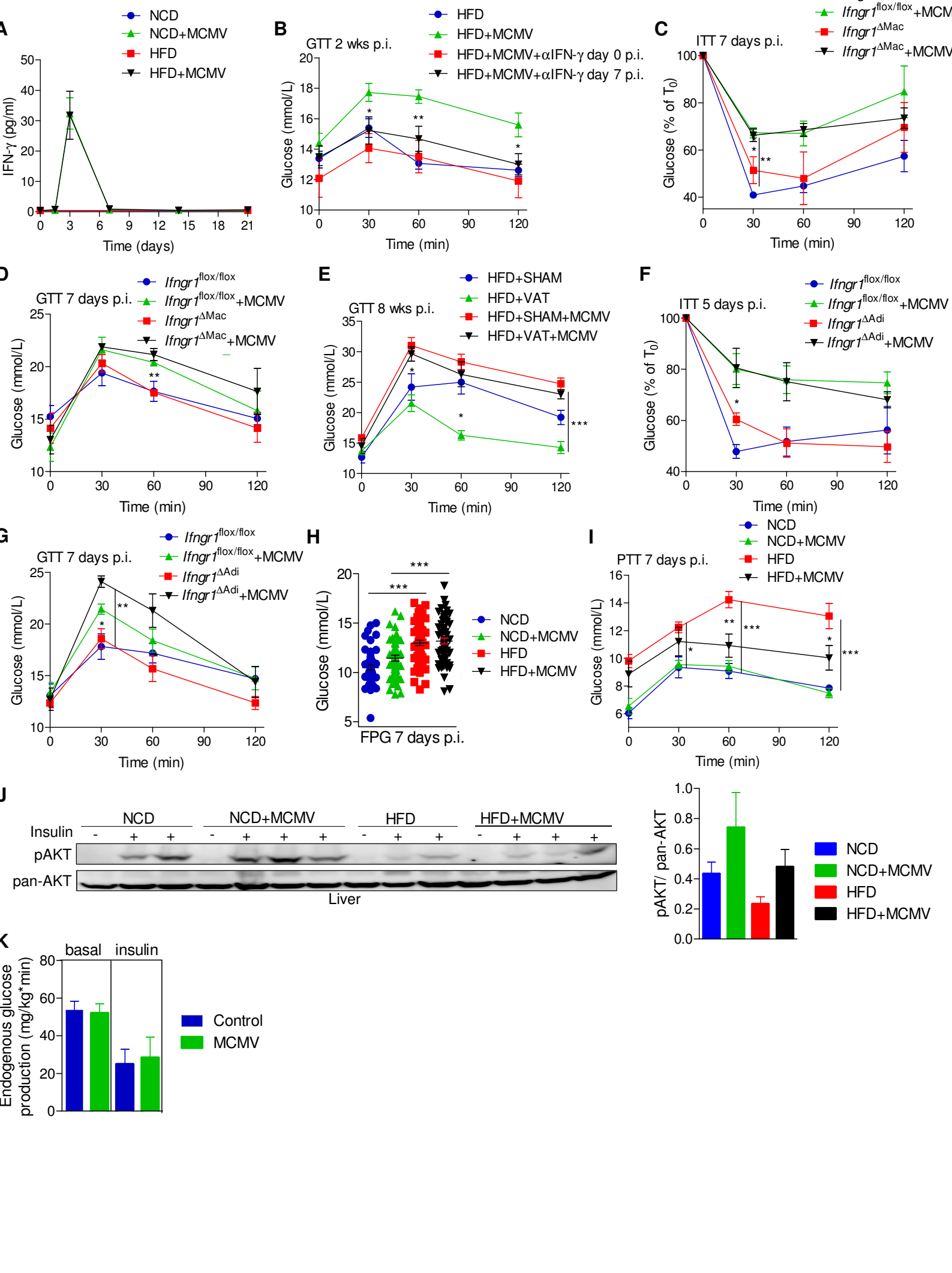
A
NCD
NCD+MCMV
HFD
HFD+MCMV
IFN-γ (pg/ml)
Time (days)
B
GTT 2 wks p.i.
HFD
HFD+MCMV
HFD+MCMV+αIFN-γ day 0 p.i.
HFD+MCMV+αIFN-γ day 7 p.i.
Glucose (mmol/L)
Time (min)
C
ITT 7 days p.i.
Ifngr1flox/flox
Ifngr1flox/flox+MCM
Ifngr1ΔMac
Ifngr1ΔMac+MCMV
Glucose (% of T0)
Time (min)
D
GTT 7 days p.i.
Ifngr1flox/flox
Ifngr1flox/flox+MCMV
Ifngr1ΔMac
Ifngr1ΔMac+MCMV
Glucose (mmol/L)
Time (min)
E
GTT 8 wks p.i.
HFD+SHAM
HFD+VAT
HFD+SHAM+MCMV
HFD+VAT+MCMV
Glucose (mmol/L)
Time (min)
F
ITT 5 days p.i.
Ifngr1flox/flox
Ifngr1flox/flox+MCMV
Ifngr1ΔAdi
Ifngr1ΔAdi+MCMV
Glucose (% of T0)
Time (min)
G
GTT 7 days p.i.
Ifngr1flox/flox
Ifngr1flox/flox+MCMV
Ifngr1ΔAdi
Ifngr1ΔAdi+MCMV
Glucose (mmol/L)
Time (min)
H
FPG 7 days p.i.
NCD
NCD+MCMV
HFD
HFD+MCMV
Glucose (mmol/L)
I
PTT 7 days p.i.
NCD
NCD+MCMV
HFD
HFD+MCMV
Glucose (mmol/L)
Time (min)
J
NCD
NCD+MCMV
HFD
HFD+MCMV
Insulin
pAKT
pan-AKT
Liver
pAKT/ pan-AKT
NCD
NCD+MCMV
HFD
HFD+MCMV
K
basal
insulin
Endogenous glucose production (mg/kg*min)
Control
MCMV

Figure 4.

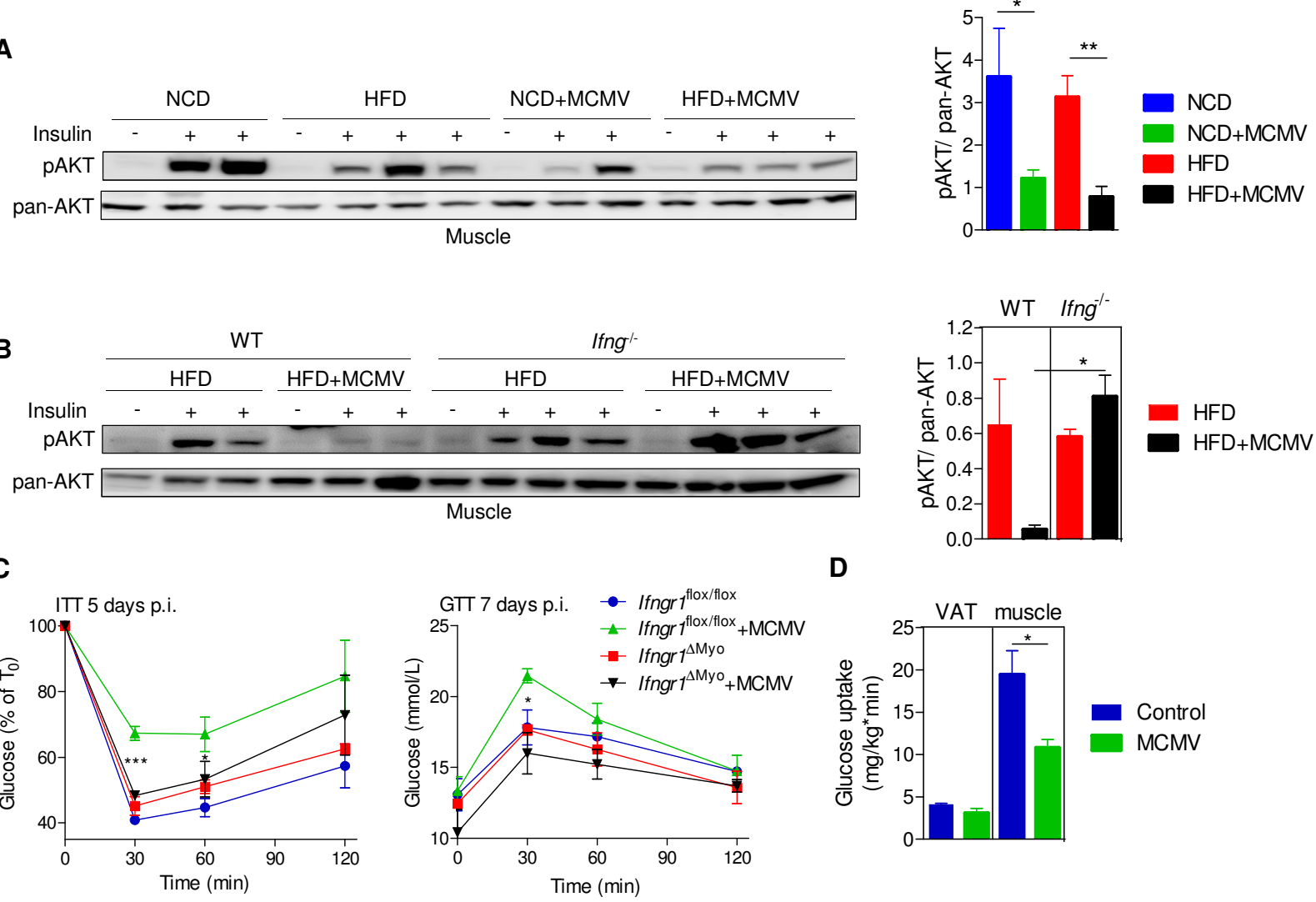
A
NCD
HFD
NCD+MCMV
HFD+MCMV
Insulin
pAKT
pan-AKT
Muscle
pAKT/ pan-AKT
NCD
NCD+MCMV
HFD
HFD+MCMV
B
WT
Ifng-/-
HFD
HFD+MCMV
Insulin
pAKT
pan-AKT
Muscle
pAKT/ pan-AKT
HFD
HFD+MCMV
C
ITT 5 days p.i.
Glucose (% of T0)
Time (min)
GTT 7 days p.i.
Ifngr1flox/flox
Ifngr1flox/flox+MCMV
Ifngr1ΔMyo
Ifngr1ΔMyo+MCMV
Glucose (mmol/L)
Time (min)
D
VAT
muscle
Glucose uptake (mg/kg*min)
Control
MCMV

Figure 5.

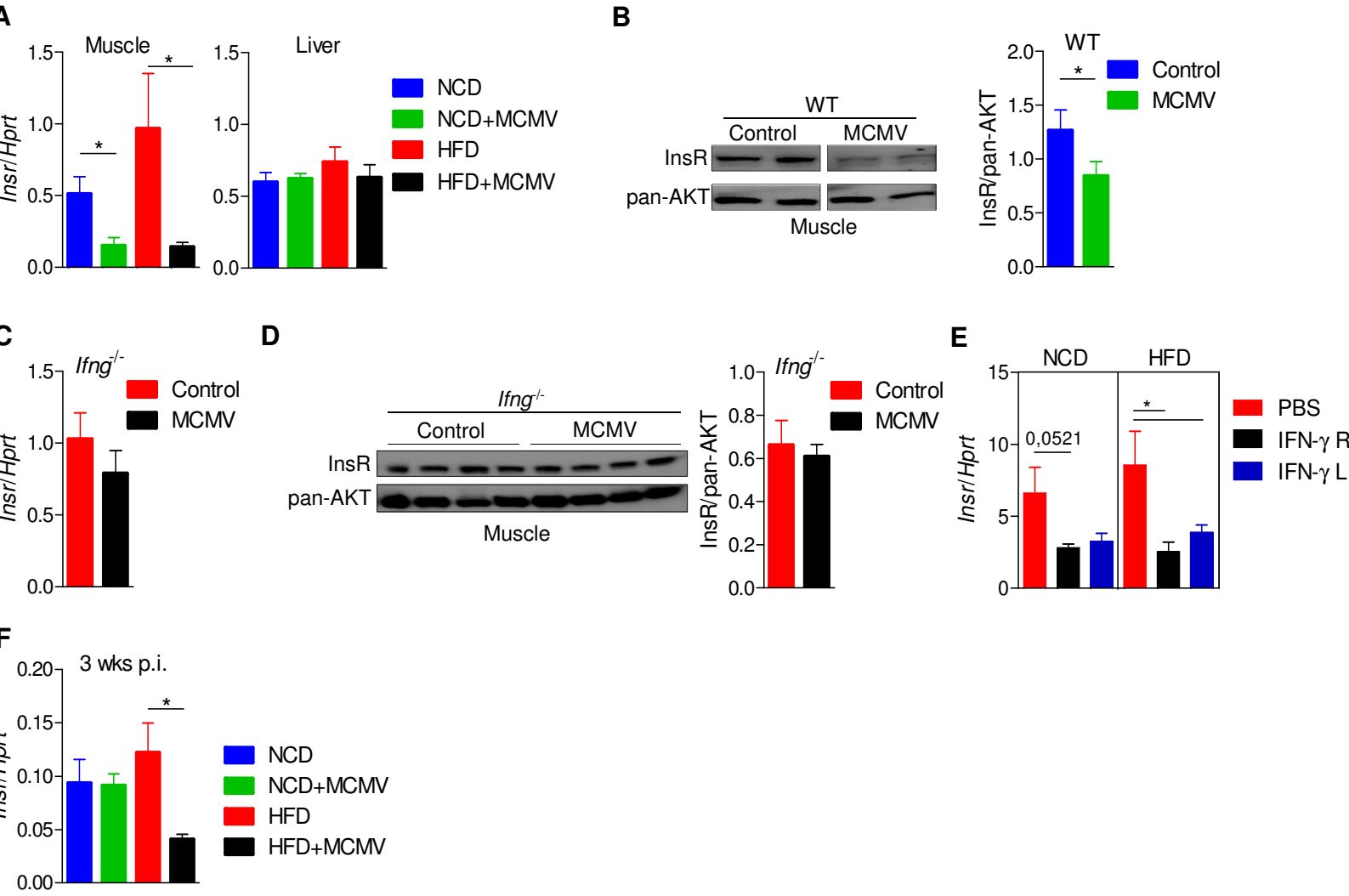
A
Muscle
Liver
Insr/Hprt
1.5
1.0
0.5
0.0
*
*
NCD
NCD+MCMV
HFD
HFD+MCMV
B
WT
Control
MCMV
InsR
pan-AKT
Muscle
WT
InsR/pan-AKT
2.0
1.5
1.0
0.5
0.0
*
Control
MCMV
C
Ifng-/-
Insr/Hprt
Control
MCMV
D
Ifng-/-
Control
MCMV
InsR
pan-AKT
Muscle
Ifng-/-
InsR/pan-AKT
1.0
0.8
0.6
0.4
0.2
0.0
Control
MCMV
E
NCD
HFD
Insr/Hprt
15
10
5
0
0,0521
*
PBS
IFN-γ R
IFN-γ L
F
3 wks p.i.
0.20
0.15
0.10
0.05
0.00
*
NCD
NCD+MCMV
HFD
HFD+MCMV

Figure 6.

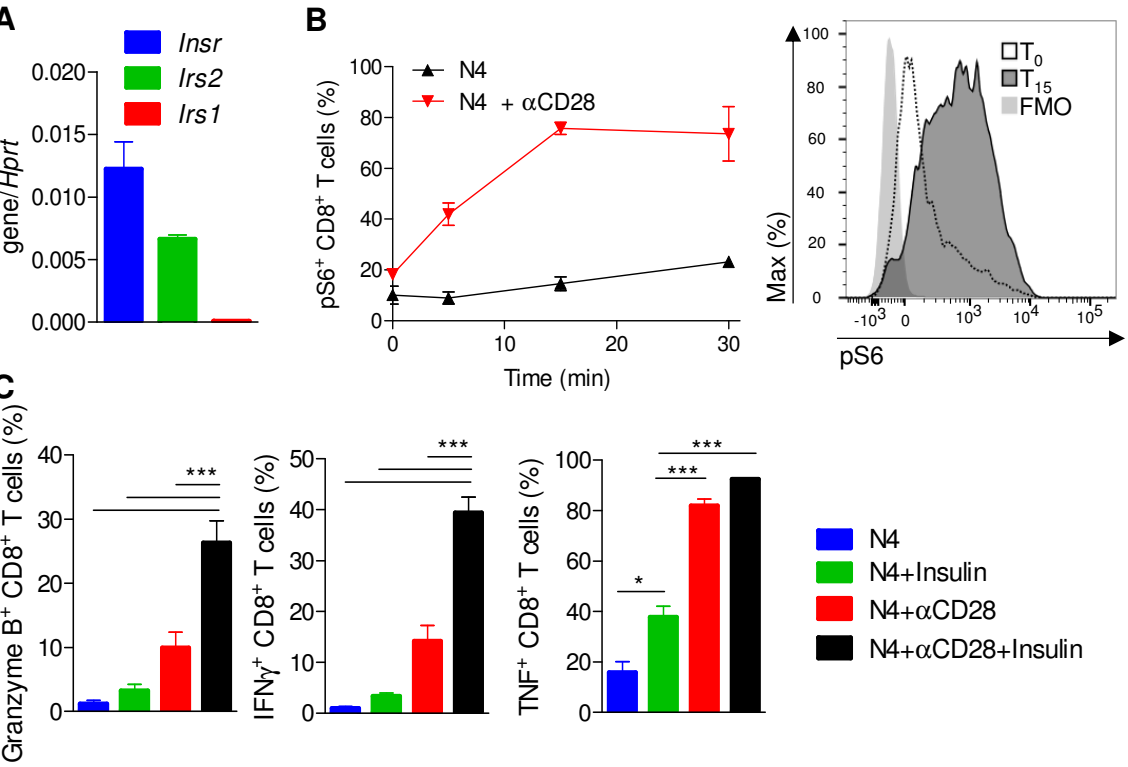
A
Insr
Irs2
Irs1
gene/Hprt
0.020
0.015
0.010
0.005
0.000
B
N4
N4 + αCD28
pS6+ CD8+ T cells (%)
Time (min)
T0
T15
FMO
Max (%)
pS6

C
Granzyme B+ CD8+ T cells (%)
IFNγ+ CD8+ T cells (%)
TNF+ CD8+ T cells (%)
***
*
N4
N4+Insulin
N4+αCD28
N4+αCD28+Insulin

Figure 7.

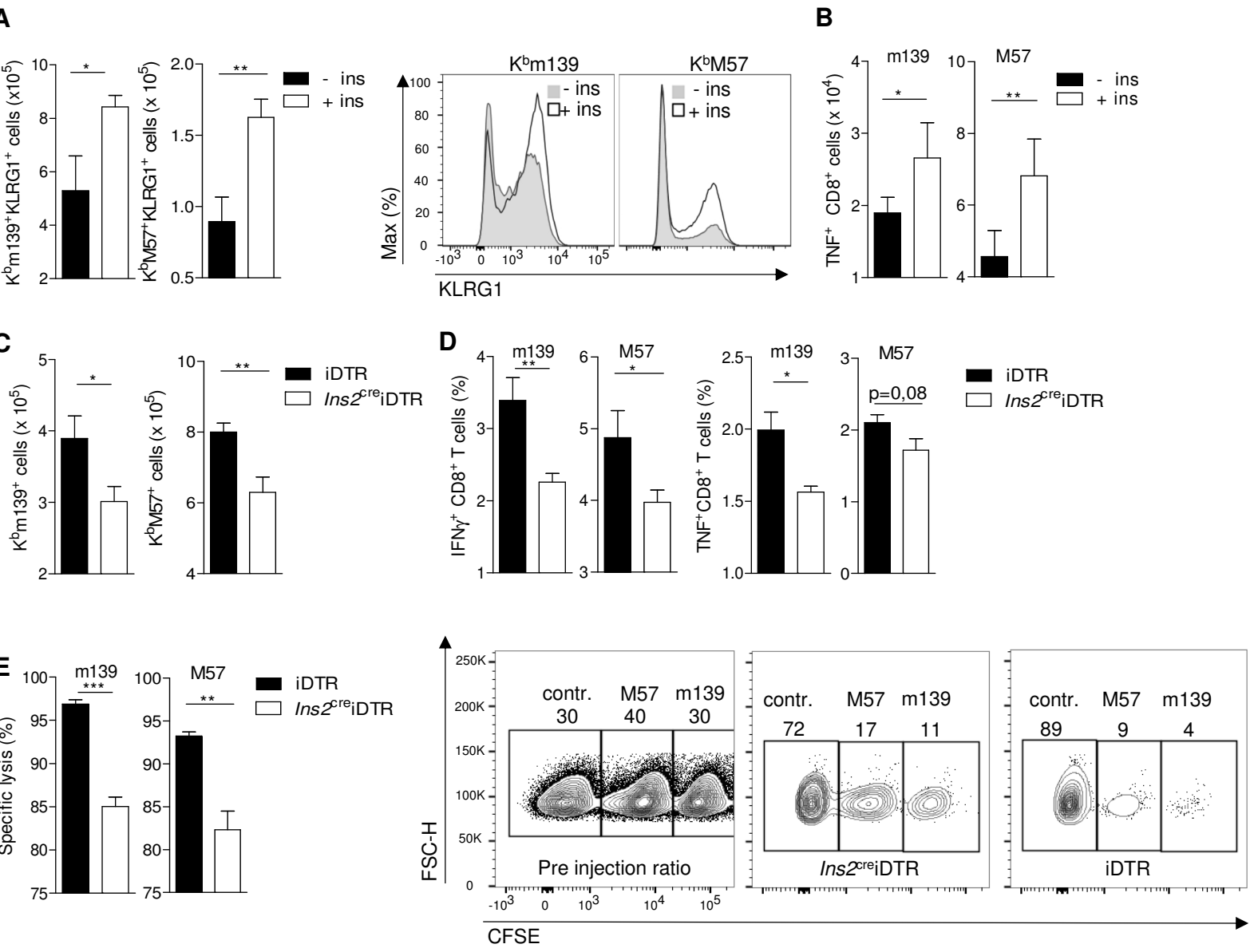
A
B
C
D
E
F
G
- ins
+ ins
iDTR
Ins2cre iDTR
m139
M57
KbM57
KLRG1
Max (%)
TNF+ CD8+ cells (x 10^4)
IFNγ+ CD8+ T cells (%)
TNF+CD8+ T cells (%)
p=0,08
Specific lysis (%)
FSC-H
CFSE
contr.
Pre injection ratio
30
40
72
17
11
89
9
4
Ifngr1flox/flox
Ifngr1ΔMyo
0.08

Supplemental Information

Virus-induced interferon-γ causes insulin resistance in skeletal muscle and derails glycemic control in obesity

Marko Šestan, Sonja Marinović, Inga Kavazović, Đurđica Cekinović, Stephan Wueest, Tamara Turk Wensveen, Ilija Brizić, Stipan Jonjić, Daniel Konrad, Felix M. Wensveen and Bojan Polić

Figure S1. Related to Figure 1. Infection promotes development of glucose intolerance and insulin resistance in pre-diabetic mice. (**A**) B6 mice were infected with MCMV or left untreated. After one, three, five, seven and twenty-one days, animals were subjected to ITT (n=5). (**B**) Blood glucose concentrations during the clamp. (**C-F**) Mice were fed for 6 weeks with NCD or HFD. (**C**) Six weeks after start of the diets, FPG was measured (n=60; pooled data of 12 experiments). (**D-F**) Six weeks after start of the diets, mice were subjected to (**D**) pyruvate tolerance test (PTT, n=5), (**E**) ITT (n=5) and (**F**) GTT (n=5). (**G**) Mice that were fed either with NCD or with HFD for 6 weeks were infected with MCVM or left untreated. One-week p.i. total body weight (n=30; pooled data of 6 experiments) or periepididymal fat pad weight (n=5) were measured. (**H, I**) Mice were fed 6 weeks with NCD or HFD and then infected with (**H**) LCMV or (**I**) Influenza A. One-week p.i. mice were subjected to GTT (n=5). (**J**) Mice were NCD or HFD fed for 6 weeks and then infected with MCMV. Three weeks p.i. MCMV (PFU) titres were determined in indicated tissues (n=4-5). (**K, L**) Mice were fed with NCD or HFD for 6 weeks and then infected with (**K**) LCMV or (**L**) Influenza A virus or left untreated. Three weeks p.i. mice were subjected to GTT (n=5). (**M**) PAS staining of kidney sections after 24 weeks of feeding. (Green arrow) expansion of mesangial matrix, (yellow arrow) increased Bowman capsule size and (red arrow) fibrin cap. (**N**) MCMV immediate early protein (IE1) staining of kidney sections 16 weeks after MCMV infection and start of HFD or NCD. (Liver control shows a section stained at day 4 after infection as a positive control). (**O**) MCMV titers (PFU) in liver of animals that were injected with PBS or ganciclovir daily, one day after infection with MCMV (n=5) are shown. (**A, D-O**). Representative of at least three experiments is shown. (**B**) The experiment was performed once. Indicated are means ± s.e.m. and statistical significances at * $p<0.05$, ** $p<0.01$, ***$p<0.001$ by (**A-F**) Student`s t test or (**G-I and K, L**) by ANOVA followed by Bonferroni post-testing and (**J**) Mann Whitney U test. LD-level of detection. PFU-plaque forming units. p.i. - post infection.

Figure S2. Related to Figure 2. Virally-induced IFN-γ promotes development of IR and GI in pre-diabetic mice. (**A-D**) Mice were NCD- or HFD-fed for 6 weeks. After 6 weeks of HFD, mice were treated with CCl_4 or paracetamol. (**A**) Representative pictures of Sirius red staining of livers sections are shown, magnification 100 x. (CCl_4 promotes development of collagen that is labeled red in Sirius red staining). (**B**) Blood concentrations of ALT after 7 days of treatment with paracetamol (n=5). (**C, D**) One week after starting with CCl_4 or paracetamol treatment mice were subjected to GTT (n=5). (**E-F**) After B6 mice were primed with HFD for 6 weeks, animals were infected with MCMV or left untreated. In addition, (**E**) mice received MCC950 (n=5) or (**F**) IL-1β (n=5) depleting antibody every second day starting one day before infection. One week p.i. mice were subjected to GTT. (**G, H**) After 6 weeks of HFD mice were injected every third day with Poly I:C. Seven days after initiating Poly I:C treatment (**G**) peritoneal macrophages were isolated and analyzed for expression of MCH class I. (**H**) mice were subjected to GTT (n=5). (**I**) *Tnfrsf1a*$^{-/-}$ mice were infected with MCMV after HFD priming for 6 weeks. GTT was performed one week p.i. (n=5). (**J**) B6 mice were infected with MCMV. In addition, mice were treated with IFN-γ neutralization antibody or isotype control every third day, starting one day before infection. Fourth and seventh days p.i. viral titers were determined in indicated tissues (n=5). (**K**) After 6 weeks of HFD priming, mice were infected with LCMV or left untreated. In addition, mice received IFN-γ depleting antibody every third day starting one day before infection. After 7 days mice were subjected to GTT (n=5). (**L**) *Ifng*$^{-/-}$ or B6 (WT) mice were fed with HFD for 6 weeks and then infected with MCMV or left untreated. One week after mice were subjected to GTT (shown is fold increase in plasma glucose concentrations compared to T_0) (n=4-5). (**M**) After infection with MCMV mice were fed with NCD of HFD for 8 weeks and received depleting NK1.1 antibody or isotype control every 5 days. After 8 weeks mice were subjected to GTT (n=5). (**N**) Mice were HFD fed for 6 weeks. After 6 weeks of HFD mice were infected with WT MCMV or Δ*m157*. One-week p.i. mice were subjected to GTT (n=5). Representative of at least three experiments is shown. Indicated are means ± s.e.m. and statistical significances at * $p<0.05$, ** $p<0.01$ and $p<0.001$*** by (**B**) Student`s t test or (**C-I, K-N**) ANOVA followed by Bonferroni post-testing. p.i. - post infection.

Figure S3. Related to Figure 3. IFN-γ induces insulin resistance independently of macrophages and hepatocytes. (**A**) Mice were infected with MCMV or left untreated and placed on NCD or HFD. M1 macrophages were quantified after 3 weeks in VAT (n=5). (**B**) Mice that were fed with HFD or NCD for 6 weeks were infected with MCMV. In addition, mice received clodronate-loaded or control liposomes one day before infection. One-week p.i. mice were subjected to GTT (n=5). (**C**) *Ifngr1*$^{\Delta Hep}$ and littermate control mice were placed on HFD for 6 weeks and then infected with MCMV or left untreated. Five days p.i. mice were subjected to ITT and 7 days p.i. to GTT (n=3-5). Representative of at least three experiments is shown. Indicated are means ± s.e.m. and statistical significances at * $p<0.05$, ** $p<0.01$, *** $p<0.001$ by ANOVA followed by Bonferroni post-testing. p.i. - post infection.

Figure S4. Related to Figure 4. Infection increases expression of IFN-γ in skeletal muscle. B6 mice were NCD or HFD fed for 6 weeks, and then infected with MCMV or left untreated. After seven days *Ifng* transcripts were determined in muscle by qPCR (n=5). Representative of two experiments with similar results is shown. Indicated are means ± s.e.m. and statistical significances at ** $p<0.01$, ***$p<0.001$ by ANOVA followed by Bonferroni post-testing

Figure S5. Related to Figure 5. IFN-γ promotes insulin resistance by downregulation of the insulin receptor. (**A-B**) B6 mice were NCD or HFD fed for 6 weeks, and then infected with MCMV or left untreated. After seven days (**A**) *Irs1*, *Irs2* or (**B**) *Socs1* and *Socs3* transcripts were determined in muscle samples by qPCR (n=4-5). (**C, D**) Lean B6 mice were infected with MCMV or left uninfected. After five days (**C**) mRNA or (**D**) protein amounts were determined in skeletal muscle samples by qPCR or immune blot, respectively (n=5). (**E**) Lean B6 mice were infected with LCMV or Influenza A virus or left uninfected. Seven days p.i. transcripts of *Insr* were determined in muscle by qPCR (normalization to uninfected animals is shown) (n=5). (**F, G**) Mice were fed for 6 weeks with NCD or HFD. After 6 weeks mouse recombinant IFN-γ or PBS was injected in right *m. sartorius* on daily basis. After 3 days, (**F**) expression of MHC class II molecules were determined on muscle tissue macrophages at the site of of IFN-γ injection. In addition, (**G**) mRNAs of the *Insr* were determined in the livers (n=5). Representative of at least three experiments is shown. Indicated are means ± s.e.m. and statistical significances at * $p<0.05$ by (**C, D**) Student`s t test or (**A, B, E, G**) ANOVA followed by Bonferroni post-testing. p.i. - post infection. InsR – insulin receptor.

Figure S6. Related to Figure 6. Insulin does not affect proliferation and viability of *in vivo* primed CD8$^+$ T cells. (**A**) OT-1 CD8 T cells were labelled with CFSE and stimulated *in vitro* with N4 peptide with or without 0.5 mg/ml αCD28, in the presence or absence of 1 U/ml of insulin. After two days CFSE dilution was measured as a read-out for proliferation. Red lines are drawn for easy analysis of differences in proliferation. (**B**) OT-1 CD8$^+$ T cells were stimulated *in vitro* with N4 peptide with or without 0.5 mg/ml αCD28, in the presence or absence of 1U/ml of insulin. After two and three days viability (Viability dye$^-$) was checked by flow cytometry. Representative of at least three experiments is shown (n=3).

Figure S7. Related to Figure 7. DT abrogates production of insulin in *Ins2*^{cre}iDTR mice. (**A, B**) *Ins2*^{cre} iDTR or iDTR littermate controls were injected twice with DT (once per day), and 24 hours later challenged with a glucose bolus after 6 hours of fasting. Before glucose administration and 30 min later (**A**) plasma insulin and (**B**) blood glucose concentrations were measured. In addition, (**C**) fold increase in blood glucose concentrations was measured 30 min after glucose administration (n=3-4). Representative of two experiments with similar results is shown. Indicated are means ± s.e.m. and statistical significance at at * $p<0.05$, ** $p<0.01$, ***$p<0.001$ by ANOVA followed by Bonferroni post-testing.

Supplemental Information

Virus-induced interferon-γ causes insulin resistance in skeletal muscle and derails glycemic control in obesity

Marko Šestan, Sonja Marinović, Inga Kavazović, Đurđica Cekinović, Stephan Wueest, Tamara Turk Wensveen, Ilija Brizić, Stipan Jonjić, Daniel Konrad, Felix M. Wensveen and Bojan Polić

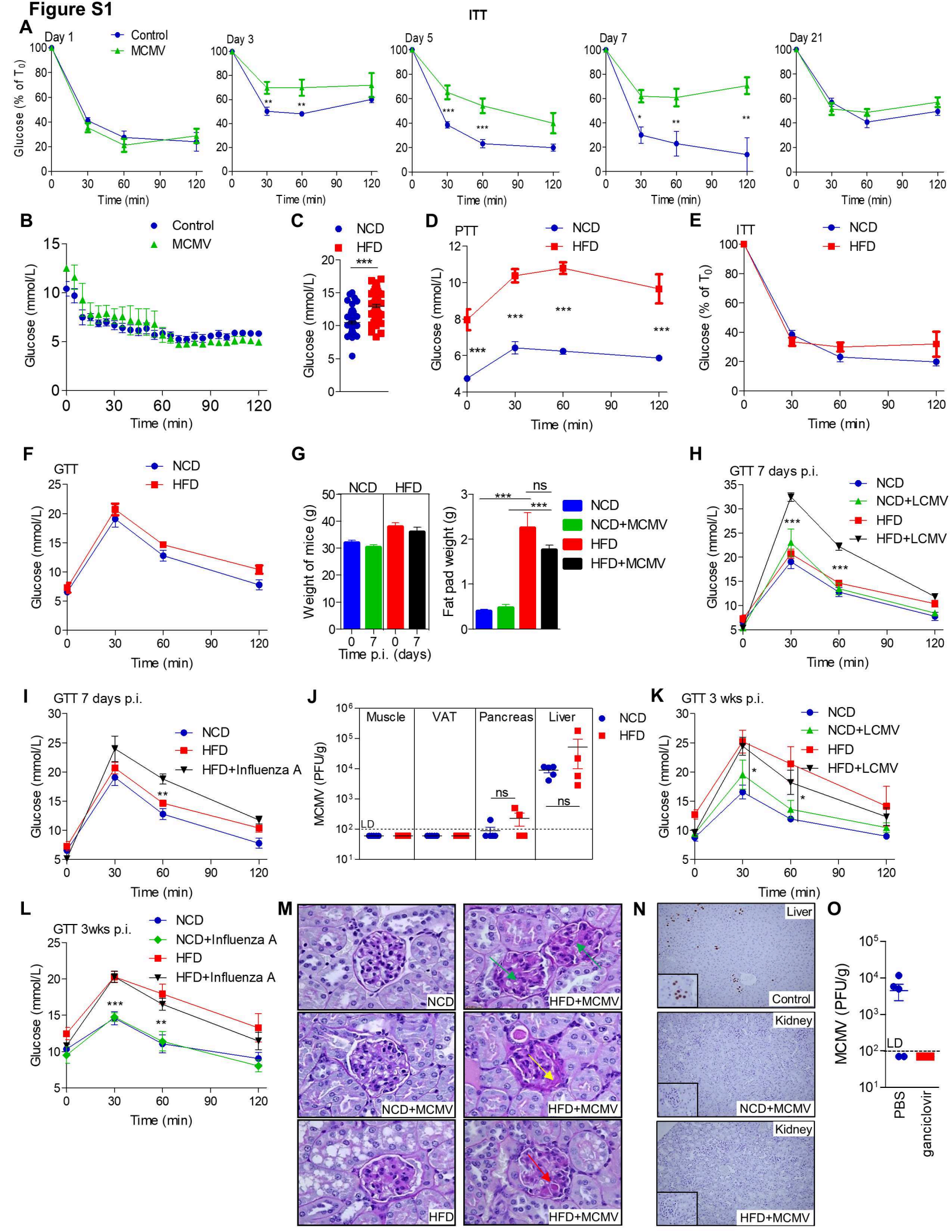
Figure S1
ITT
A
Day 1
Day 3
Day 5
Day 7
Day 21
Control
MCMV
Glucose (% of T0)
Time (min)
B
Control
MCMV
Glucose (mmol/L)
Time (min)
C
NCD
HFD
Glucose (mmol/L)
D
PTT
NCD
HFD
Glucose (mmol/L)
Time (min)
E
ITT
NCD
HFD
Glucose (% of T0)
Time (min)
F
GTT
NCD
HFD
Glucose (mmol/L)
Time (min)
G
NCD
HFD
Weight of mice (g)
Time p.i. (days)
Fat pad weight (g)
ns
NCD
NCD+MCMV
HFD
HFD+MCMV
H
GTT 7 days p.i.
NCD
NCD+LCMV
HFD
HFD+LCMV
Glucose (mmol/L)
Time (min)
I
GTT 7 days p.i.
NCD
HFD
HFD+Influenza A
Glucose (mmol/L)
Time (min)
J
Muscle
VAT
Pancreas
Liver
NCD
HFD
MCMV (PFU/g)
LD
ns
K
GTT 3 wks p.i.
NCD
NCD+LCMV
HFD
HFD+LCMV
Glucose (mmol/L)
Time (min)
L
GTT 3wks p.i.
NCD
NCD+Influenza A
HFD
HFD+Influenza A
Glucose (mmol/L)
Time (min)
M
NCD
HFD+MCMV
NCD+MCMV
HFD+MCMV
HFD
HFD+MCMV
N
Liver
Control
Kidney
NCD+MCMV
Kidney
HFD+MCMV
O
MCMV (PFU/g)
LD
PBS
ganciclovir

Figure S1. Related to Figure 1. Infection promotes development of glucose intolerance and insulin resistance in pre-diabetic mice. (**A**) B6 mice were infected with MCMV or left untreated. After one, three, five, seven and twenty-one days, animals were subjected to ITT (n=5). (**B**) Blood glucose concentrations during the clamp. (**C-F**) Mice were fed for 6 weeks with NCD or HFD. (**C**) Six weeks after start of the diets, FPG was measured (n=60; pooled data of 12 experiments). (**D-F**) Six weeks after start of the diets, mice were subjected to (**D**) pyruvate tolerance test (PTT, n=5), (**E**) ITT (n=5) and (**F**) GTT (n=5). (**G**) Mice that were fed either with NCD or with HFD for 6 weeks were infected with MCVM or left untreated. One-week p.i. total body weight (n=30; pooled data of 6 experiments) or periepididymal fat pad weight (n=5) were measured. (**H, I**) Mice were fed 6 weeks with NCD or HFD and then infected with (**H**) LCMV or (**I**) Influenza A. One-week p.i. mice were subjected to GTT (n=5). (**J**) Mice were NCD or HFD fed for 6 weeks and then infected with MCMV. Three weeks p.i. MCMV (PFU) titres were determined in indicated tissues (n=4-5). (**K, L**) Mice were fed with NCD or HFD for 6 weeks and then infected with (**K**) LCMV or (**L**) Influenza A virus or left untreated. Three weeks p.i. mice were subjected to GTT (n=5). (**M**) PAS staining of kidney sections after 24 weeks of feeding. (Green arrow) expansion of mesangial matrix, (yellow arrow) increased Bowman capsule size and (red arrow) fibrin cap. (**N**) MCMV immediate early protein (IE1) staining of kidney sections 16 weeks after MCMV infection and start of HFD or NCD. (Liver control shows a section stained at day 4 after infection as a positive control). (**O**) MCMV titers (PFU) in liver of animals that were injected with PBS or ganciclovir daily, one day after infection with MCMV (n=5) are shown. (**A, D-O**). Representative of at least three experiments is shown. (**B**) The experiment was performed once. Indicated are means ± s.e.m. and statistical significances at * $p<0.05$, ** $p<0.01$, *** $p<0.001$ by (**A-F**) Student`s t test or (**G-I and K, L**) by ANOVA followed by Bonferroni post-testing and (**J**) Mann Whitney U test. LD-level of detection. PFU-plaque forming units. p.i. - post infection.

Figure S2.

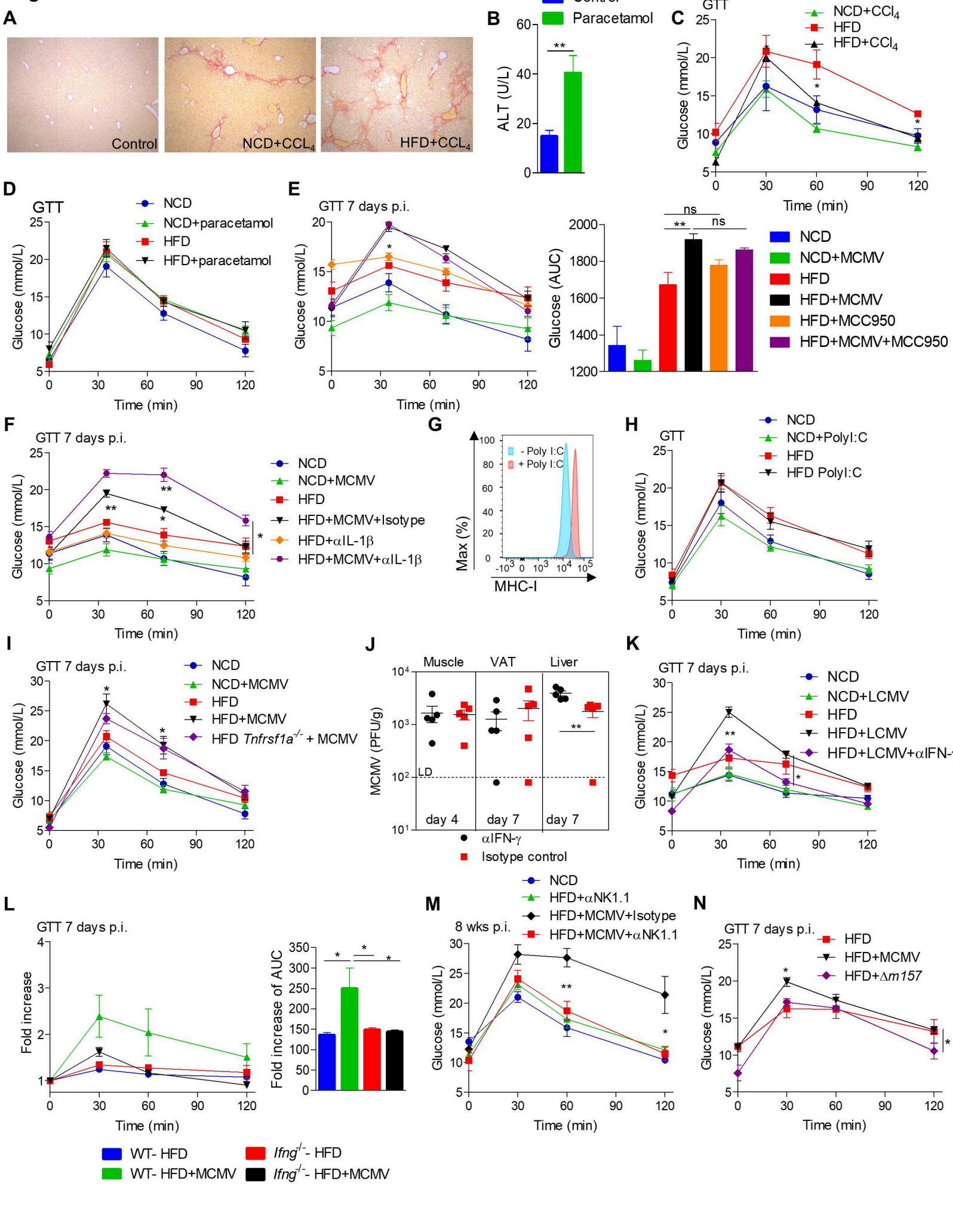
A
Control
NCD+CCL4
HFD+CCL4
B
Control
Paracetamol
ALT (U/L)
C
GTT
NCD
NCD+CCl4
HFD
HFD+CCl4
Glucose (mmol/L)
Time (min)
D
GTT
NCD
NCD+paracetamol
HFD
HFD+paracetamol
E
GTT 7 days p.i.
Glucose (AUC)
NCD
NCD+MCMV
HFD
HFD+MCMV
HFD+MCC950
HFD+MCMV+MCC950
F
GTT 7 days p.i.
HFD+MCMV+Isotype
HFD+αIL-1β
HFD+MCMV+αIL-1β
G
- Poly I:C
+ Poly I:C
Max (%)
MHC-I
H
GTT
NCD+PolyI:C
HFD PolyI:C
I
GTT 7 days p.i.
HFD Tnfrsf1a-/- + MCMV
J
Muscle
VAT
Liver
MCMV (PFU/g)
LD
day 4
day 7
day 7
αIFN-γ
Isotype control
K
GTT 7 days p.i.
NCD+LCMV
HFD+LCMV
HFD+LCMV+αIFN-γ
L
GTT 7 days p.i.
Fold increase
Fold increase of AUC
WT- HFD
WT- HFD+MCMV
Ifng-/- - HFD
Ifng-/- - HFD+MCMV
M
8 wks p.i.
HFD+αNK1.1
HFD+MCMV+Isotype
HFD+MCMV+αNK1.1
N
GTT 7 days p.i.
HFD+Δm157
Time (min)

Figure S2. Related to Figure 2. Virally-induced IFN-γ promotes development of IR and GI in pre-diabetic mice. (**A-D**) Mice were NCD- or HFD-fed for 6 weeks. After 6 weeks of HFD, mice were treated with CCl_4 or paracetamol. (**A**) Representative pictures of Sirius red staining of livers sections are shown, magnification 100 x. (CCl_4 promotes development of collagen that is labeled red in Sirius red staining). (**B**) Blood concentrations of ALT after 7 days of treatment with paracetamol (n=5). (**C, D**) One week after starting with CCl_4 or paracetamol treatment mice were subjected to GTT (n=5). (**E-F**) After B6 mice were primed with HFD for 6 weeks, animals were infected with MCMV or left untreated. In addition, (**E**) mice received MCC950 (n=5) or (**F**) IL-1β (n=5) depleting antibody every second day starting one day before infection. One week p.i. mice were subjected to GTT. (**G, H**) After 6 weeks of HFD mice were injected every third day with Poly I:C. Seven days after initiating Poly I:C treatment (**G**) peritoneal macrophages were isolated and analyzed for expression of MCH class I. (**H**) mice were subjected to GTT (n=5). (**I**) *Tnfrsf1a*$^{-/-}$ mice were infected with MCMV after HFD priming for 6 weeks. GTT was performed one week p.i. (n=5). (**J**) B6 mice were infected with MCMV. In addition, mice were treated with IFN-γ neutralization antibody or isotype control every third day, starting one day before infection. Fourth and seventh days p.i. viral titers were determined in indicated tissues (n=5). (**K**) After 6 weeks of HFD priming, mice were infected with LCMV or left untreated. In addition, mice received IFN-γ depleting antibody every third day starting one day before infection. After 7 days mice were subjected to GTT (n=5). (**L**) *Ifng*$^{-/-}$ or B6 (WT) mice were fed with HFD for 6 weeks and then infected with MCMV or left untreated. One week after mice were subjected to GTT (shown is fold increase in plasma glucose concentrations compared to T_0) (n=4-5). (**M**) After infection with MCMV mice were fed with NCD of HFD for 8 weeks and received depleting NK1.1 antibody or isotype control every 5 days. After 8 weeks mice were subjected to GTT (n=5). (**N**) Mice were HFD fed for 6 weeks. After 6 weeks of HFD mice were infected with WT MCMV or Δ*m157*. One-week p.i. mice were subjected to GTT (n=5). Representative of at least three experiments is shown. Indicated are means ± s.e.m. and statistical significances at * $p<0.05$, ** $p<0.01$ and $p<0.001$*** by (**B**) Student`s t test or (**C-I, K-N**) ANOVA followed by Bonferroni post-testing. p.i. - post infection.

Figure S3.

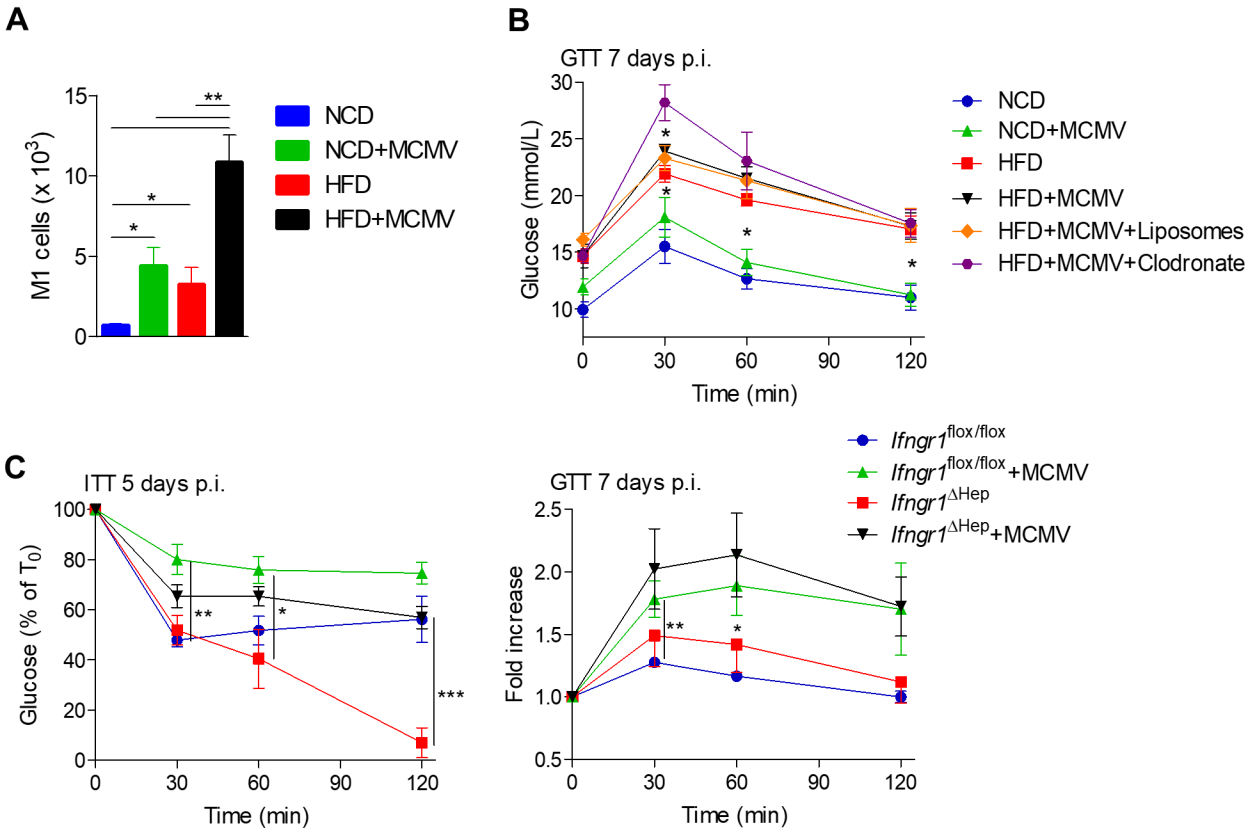
A
M1 cells (x 10^3)
NCD
NCD+MCMV
HFD
HFD+MCMV
B
GTT 7 days p.i.
Glucose (mmol/L)
Time (min)
NCD
NCD+MCMV
HFD
HFD+MCMV
HFD+MCMV+Liposomes
HFD+MCMV+Clodronate
C
ITT 5 days p.i.
Glucose (% of T0)
Time (min)
GTT 7 days p.i.
Fold increase
Time (min)
Ifngr1flox/flox
Ifngr1flox/flox+MCMV
Ifngr1ΔHep
Ifngr1ΔHep+MCMV

Figure S3. Related to Figure 3. IFN-γ induces insulin resistance independently of macrophages and hepatocytes. (**A**) Mice were infected with MCMV or left untreated and placed on NCD or HFD. M1 macrophages were quantified after 3 weeks in VAT (n=5). (**B**) Mice that were fed with HFD or NCD for 6 weeks were infected with MCMV. In addition, mice received clodronate-loaded or control liposomes one day before infection. One-week p.i. mice were subjected to GTT (n=5). (**C**) *Ifngr1*$^{\Delta Hep}$ and littermate control mice were placed on HFD for 6 weeks and then infected with MCMV or left untreated. Five days p.i. mice were subjected to ITT and 7 days p.i. to GTT (n=3-5). Representative of at least three experiments is shown. Indicated are means ± s.e.m. and statistical significances at * $p<0.05$, ** $p<0.01$, *** $p<0.001$ by ANOVA followed by Bonferroni post-testing. p.i. - post infection.

Figure S4.

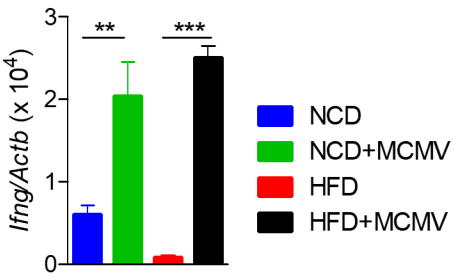

Figure S4. Related to Figure 4. Infection increases expression of IFN-γ in skeletal muscle. B6 mice were NCD or HFD fed for 6 weeks, and then infected with MCMV or left untreated. After seven days *Ifng* transcripts were determined in muscle by qPCR (n=5). Representative of two experiments with similar results is shown. Indicated are means ± s.e.m. and statistical significances at ** $p<0.01$, ***$p<0.001$ by ANOVA followed by Bonferroni post-testing

Figure S5.

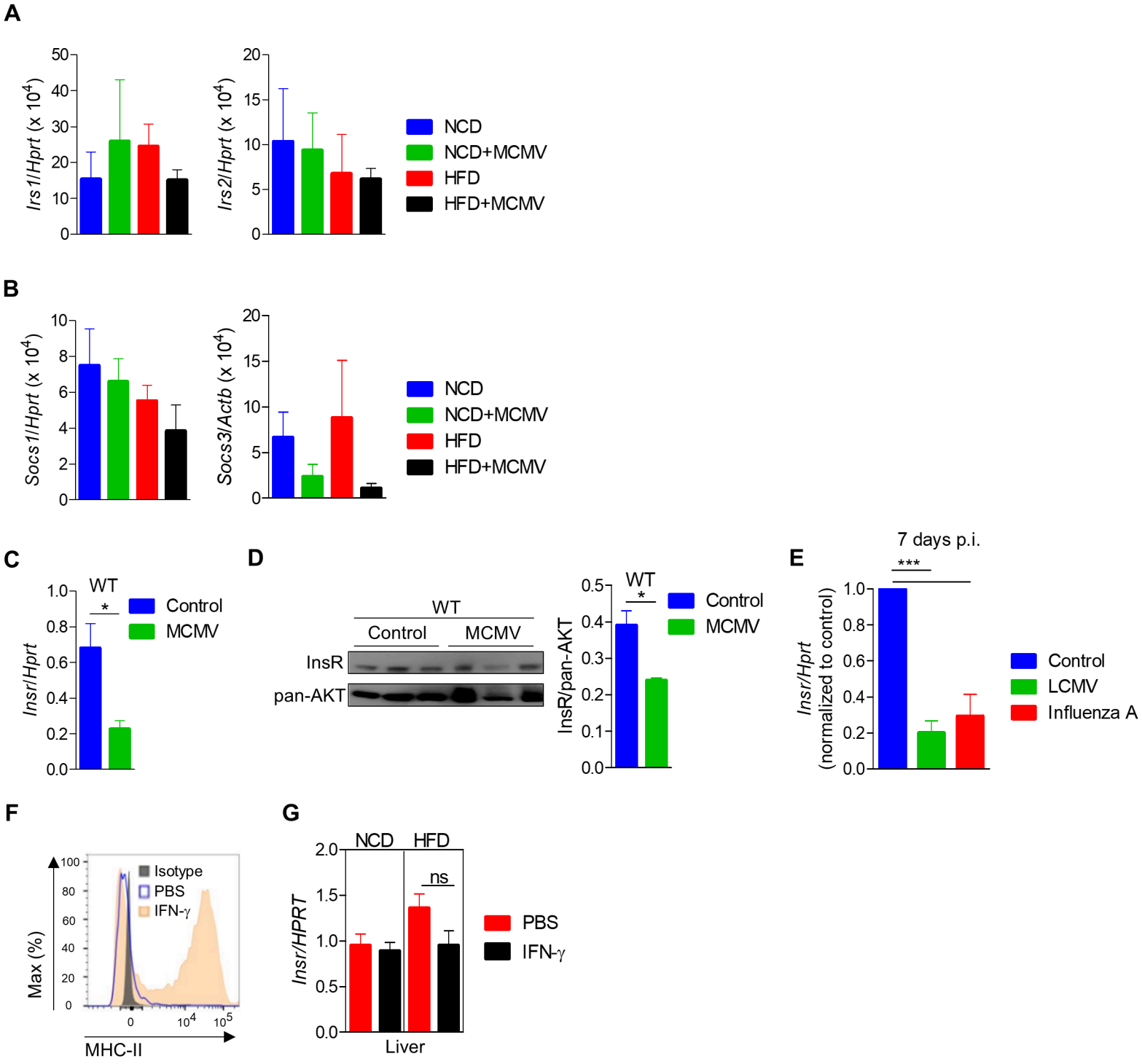
A
Irs1/Hprt (x 10^4)
Irs2/Hprt (x 10^4)
NCD
NCD+MCMV
HFD
HFD+MCMV
B
Socs1/Hprt (x 10^4)
Socs3/Actb (x 10^4)
NCD
NCD+MCMV
HFD
HFD+MCMV
C
WT
Control
MCMV
Insr/Hprt
D
WT
Control
MCMV
InsR
pan-AKT
InsR/pan-AKT
E
7 days p.i.
Insr/Hprt (normalized to control)
Control
LCMV
Influenza A
F
Isotype
PBS
IFN-γ
Max (%)
MHC-II
G
NCD
HFD
ns
Insr/HPRT
PBS
IFN-γ
Liver

Figure S5. Related to Figure 5. IFN-γ promotes insulin resistance by downregulation of the insulin receptor. (**A-B**) B6 mice were NCD or HFD fed for 6 weeks, and then infected with MCMV or left untreated. After seven days (**A**) *Irs1*, *Irs2* or (**B**) *Socs1* and *Socs3* transcripts were determined in muscle samples by qPCR (n=4-5). (**C, D**) Lean B6 mice were infected with MCMV or left uninfected. After five days (**C**) mRNA or (**D**) protein amounts were determined in skeletal muscle samples by qPCR or immune blot, respectively (n=5). (**E**) Lean B6 mice were infected with LCMV or Influenza A virus or left uninfected. Seven days p.i. transcripts of *Insr* were determined in muscle by qPCR (normalization to uninfected animals is shown) (n=5). (**F, G**) Mice were fed for 6 weeks with NCD or HFD. After 6 weeks mouse recombinant IFN-γ or PBS was injected in right *m. sartorius* on daily basis. After 3 days, (**F**) expression of MHC class II molecules were determined on muscle tissue macrophages at the site of of IFN-γ injection. In addition, (**G**) mRNAs of the *Insr* were determined in the livers (n=5). Representative of at least three experiments is shown. Indicated are means ± s.e.m. and statistical significances at * $p<0.05$ by (**C, D**) Student`s t test or (**A, B, E, G**) ANOVA followed by Bonferroni post-testing. p.i. - post infection. InsR – insulin receptor.

Figure S6.

A

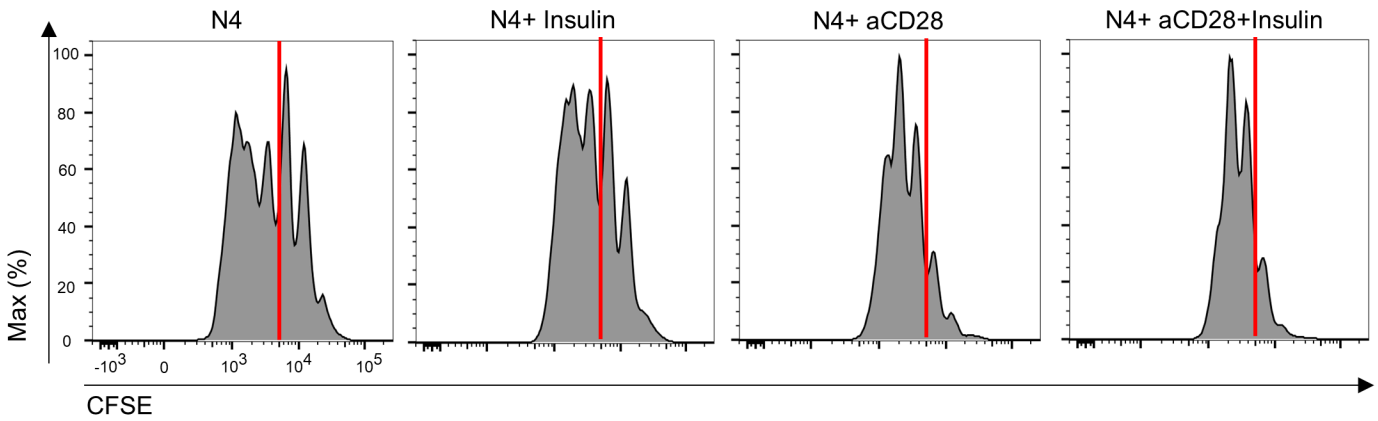
N4
N4+ Insulin
N4+ aCD28
N4+ aCD28+Insulin
Max (%)
100
80
60
40
20
0
-10^3
0
10^3
10^4
10^5
CFSE

B

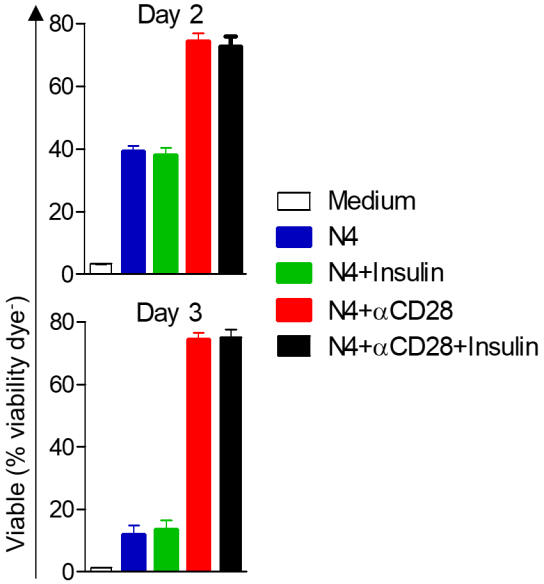
Day 2
Day 3
80
60
40
20
0
Viable (% viability dye-)
Medium
N4
N4+Insulin
N4+αCD28
N4+αCD28+Insulin

Figure S6. Related to Figure 6. Insulin does not affect proliferation and viability of *in vivo* primed CD8$^+$ T cells. (**A**) OT-1 CD8 T cells were labelled with CFSE and stimulated *in vitro* with N4 peptide with or without 0.5 mg/ml αCD28, in the presence or absence of 1 U/ml of insulin. After two days CFSE dilution was measured as a read-out for proliferation. Red lines are drawn for easy analysis of differences in proliferation. (**B**) OT-1 CD8$^+$ T cells were stimulated *in vitro* with N4 peptide with or without 0.5 mg/ml αCD28, in the presence or absence of 1U/ml of insulin. After two and three days viability (Viability dye$^-$) was checked by flow cytometry. Representative of at least three experiments is shown (n=3).

Figure S7.

A

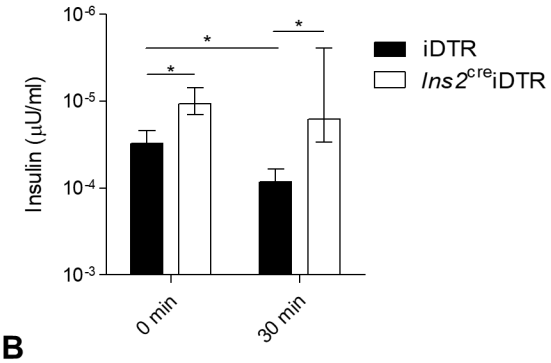

B

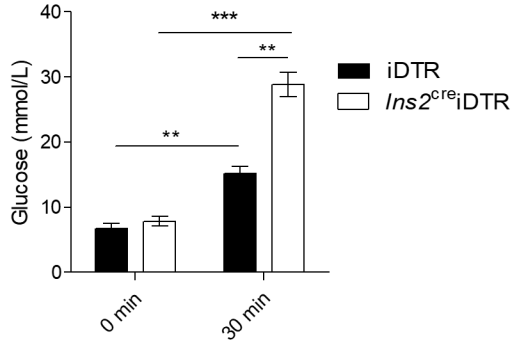

C

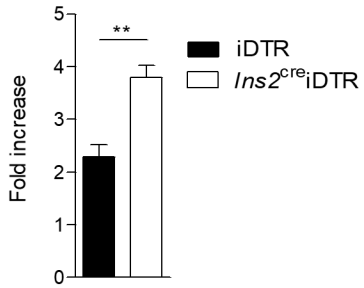

Figure S7. Related to Figure 7. DT abrogates production of insulin in *Ins2*^{cre}iDTR mice. (**A, B**) *Ins2*^{cre} iDTR or iDTR littermate controls were injected twice with DT (once per day), and 24 hours later challenged with a glucose bolus after 6 hours of fasting. Before glucose administration and 30 min later (**A**) plasma insulin and (**B**) blood glucose concentrations were measured. In addition, (**C**) fold increase in blood glucose concentrations was measured 30 min after glucose administration (n=3-4). Representative of two experiments with similar results is shown. Indicated are means ± s.e.m. and statistical significance at at * $p<0.05$, ** $p<0.01$, ***$p<0.001$ by ANOVA followed by Bonferroni post-testing.